Accepted Manuscript

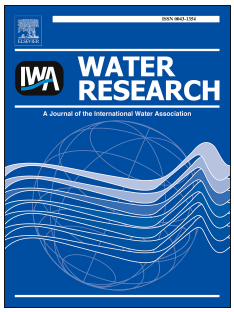

N_2 yields from monochloramine conversion by granular activated carbons are decisive for effective swimming pool water treatment

Bertram Skibinski, Eckhard Worch, Wolfgang Uhl

PII: S0043-1354(18)30997-7

DOI: https://doi.org/10.1016/j.watres.2018.11.068

Reference: WR 14275

To appear in: *Water Research*

Received Date: 28 May 2018

Revised Date: 21 November 2018

Accepted Date: 26 November 2018

Please cite this article as: Skibinski, B., Worch, E., Uhl, W., N_2 yields from monochloramine conversion by granular activated carbons are decisive for effective swimming pool water treatment, *Water Research*, https://doi.org/10.1016/j.watres.2018.11.068.

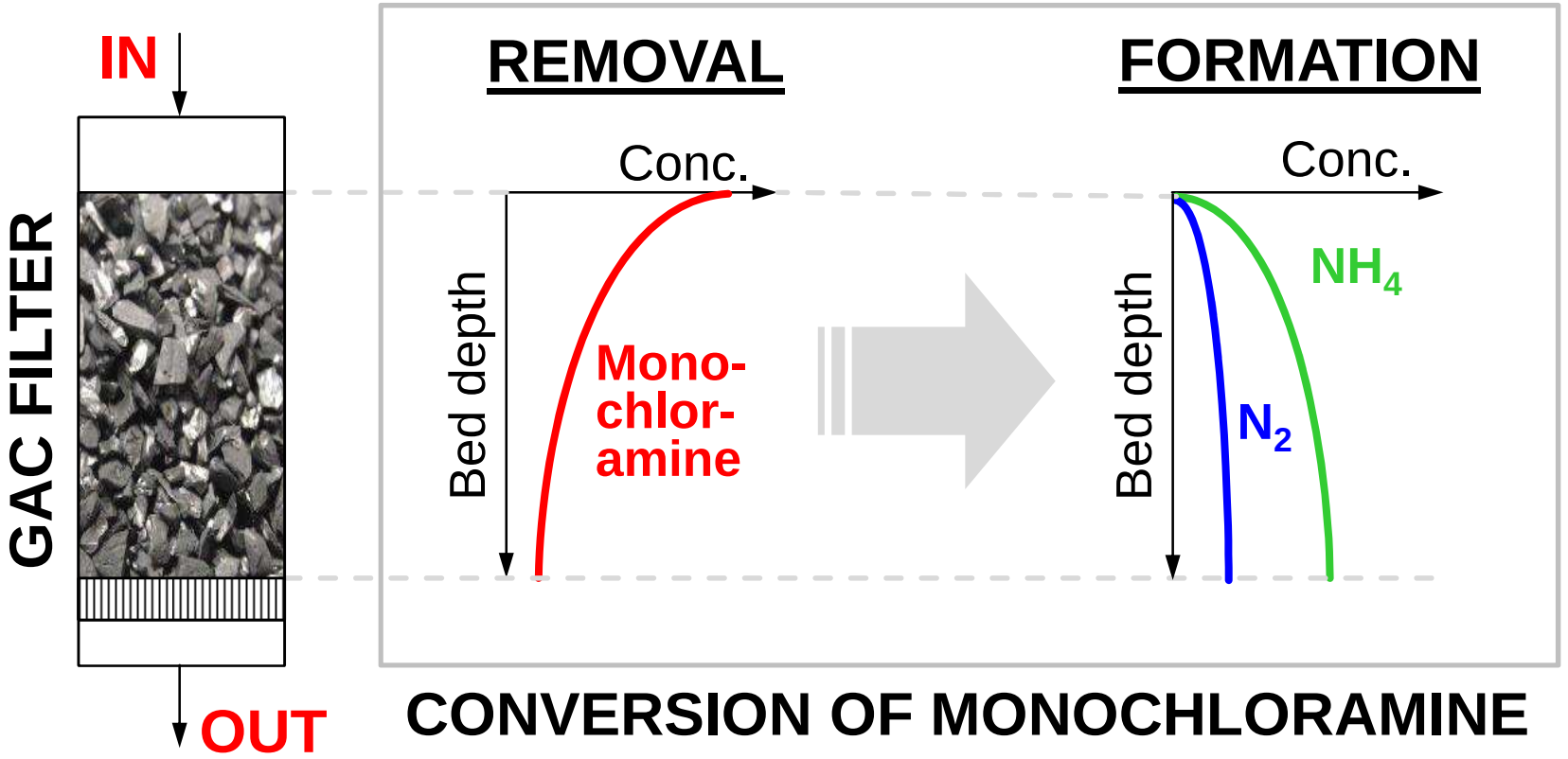

CONVERSION OF MONOCHLORAMINE

CARBON PROPERTIES

SURFACE OXIDES, TRACE ELEMENTS, C, H, N, S CONTENT, ZETA POTENTIAL

POOL WATER QUALITY

COMBINED CHLORINE, AMMONIUM, NDMA

N_2 YIELDS FROM MONOCHLORAMINE CONVERSION BY GRANULAR ACTIVATED CARBONS ARE DECISIVE FOR EFFECTIVE SWIMMING POOL WATER TREATMENT

Bertram Skibinski[1,*], Eckhard Worch[2], Wolfgang Uhl[1,3,4,*]

[1] Technische Universität Dresden, Chair of Water Supply Engineering, 01062 Dresden, Germany.

[2] Technische Universität Dresden, Chair of Hydrochemistry, 01062 Dresden, Germany.

[3] Norwegian Institute for Water Research (NIVA), 0349 Oslo, Norway.

[4] Norwegian University of Science and Technology (NTNU), Institute of Civil and Environmental Engineering, 7491 Trondheim, Norway.

* Corresponding authors. E-mail addresses:

bertram.skibinski@tu-dresden.de (Bertram Skibinski)

wolfgang.uhl@niva.no (Wolfgang Uhl)

Key words: swimming pool water; monochloramine; combined chlorine granular activated carbon; catalytic reaction; surface reaction;

Type of article: Research Paper

Abstract

Inorganic chloramines (mono-, di- and trichloramine) are formed in swimming pool water from the unintended reaction of free chlorine with ammonia that is introduced by bathers. Monochloramine is of particular interest as it is known to react further in pool water forming harmful DBPs, such carcinogenic N-nitrosodimethylamine (NDMA). During pool water treatment with granular activated carbon (GAC) filters, monochloramine is transformed by chemical reactions on the carbon surface to N_2 and ammonia. As ammonia is led back into the pool where it is chlorinated again under the renewed formation of inorganic chloramines, it is recommended to use GACs with a high N_2 yield for monochloramine transformation in pool water treatment.

In this study, yields of N_2 and ammonia from monochloramine conversion by commercially available GACs were determined using a fixed-bed reactor system under conditions that are typical for swimming pool water treatment. The N_2 yields remained constant with on-going exposure of the GAC to monochloramine and ranged from 0.5% to 21.3%, depending on the type of GAC used. Correlation analyses were conducted to identify carbon properties that can determine the N_2 yield for monochloramine conversion, such as the amount of oxygen groups, the elemental composition and the trace metal content. It was found that the N_2 yield significantly correlates with the copper content of the tested carbons.

Model calculations combining pool hydraulics with formation/abatement of inorganic chloramines and NDMA as well as chloramine transformations in GAC filters showed that the concentration of inorganic chloramines and carcinogenic NDMA can be

45 decreased by a factor of ~2, if the tested GACs could be modified to convert up to

46 ~50 % of the monochloramine to N_2.

1 Introduction and Objectives

In public swimming pools, chlorine is usually the primary disinfectant. According to national and international regulations (e.g., DIN 19643-1, 2012; ANSI/APSP-11-2009, 2009; WHO, 2006), the concentration of free chlorine has to be kept within a certain concentration range. Chlorine reacts with organic and inorganic substances introduced by bathers (Keuten et al., 2012, 2014), to form organic and inorganic disinfection by-products (DBPs) (Zwiener et al., 2007). The reaction of free chlorine with ammonia (Weil and Morris, 1949; Isaac and Morris, 1983; Qiang and Adams, 2004) and urea (Blatchley and Cheng, 2010) leads to the formation of inorganic chloramines (mono-, di- and trichloramine) in swimming pool water. Among the variety of known disinfection by-products, the occurrence and toxicological relevance of di- and trichloramine is frequently studied and discussed in the literature (Isaac and Morris, 1983; Blatchley and Cheng, 2010; Schmalz et al., 2011). Especially trichloramine has been found to cause respiratory problems, and there is evidence that it increases the risk of asthma for children during adolescence (Bernard et al., 2003, 2008).

At the neutral pH of swimming pool water, monochloramine is known to be the most dominant species among the inorganic chloramines (Weaver et al., 2009) that are monitored in swimming pool water on a regular basis as a component of the sum parameter “combined chlorine”. Concentrations of monochloramine in pool water are reported to be up to 1.88 mg L^{-1} (as Cl_2) (Weaver et al., 2009). Monochloramine is suspected to have a major role in causing irritation of the eyes and respiratory tract while bathing (Eichelsdörfer, et al., 1975). Further, oxidation of organic matter by monochloramine was found to cause the formation of other unidentified DBPs that may contain a substantial amount of toxicologically important compounds (Hua and

Reckhow, 2007). For instance, monochloramine received particular attention as it was found to react in pool water with dimethylamine (DMA), forming highly carcinogenic N-nitrosodimethylamine (NDMA) (Mitch and Sedlak, 2002; Choi and Valentine, 2002; Schreiber and Mitch, 2006). Consequently, the concentration of inorganic chloramines in pool water is subject to continuous surveillance and is strictly regulated to a concentration of <0.2 mg L^{-1} (as Cl_2) in swimming pools in Europe and the U.S. (e.g., WHO, 2006, ANSI/APSP-11-2009, 2009; SIA 385/9, 2011; DIN 19643-1, 2012).

Swimming pool water is circulated in a closed loop over a treatment section to remove chemical and microbial contaminants such as DBPs (i.e. chlormaines) and precursors to DBPs (Judd and Black, 2000; DIN 19643-1, 2012). In pool water treatment processes, granular activated carbon (GAC) filtration is used for the adsorptive removal of these contaminants (Worch, 2012). As alternatives to GAC filtration, previous studies introduce microbial treatment methods to remove harmful substances, such as nitrogen containing chloramines (Ge et al., 2015; Zhang et al., 2015). However, microbiological water treatment is not commonly used in pool water treatment due to the increased risks for the spread of waterborne infections in the closed pool water cycle. GAC filters, for instance, are backwashed with chlorine solution to mitigate microbiological growth (Uhl and Hartmann, 2005).

GAC filtration has further been known to remove mono-, di- and trichloramine by a chemical reaction at the carbon surface (Bauer and Snoeyink, 1973; Scaramelli and Digiano, 1977; Kochany and Lipczynska-Kochany, 2008; Sakuma et al., 2015). Previous studies showed that monochloramine is chemically reduced at the surface of activated carbons to ammonia (NH_3) or ammonium ion (NH_4^+) (Equation 1). A second mechanism was proposed by Bauer and Snoeyink (1973), who concluded on

a chemical reaction of monochloramine with surface oxides C^*O to form N_2 according to Equation 2. Until now, no direct evidence for the oxidative decomposition of monochloramine to N_2 according to Equation 2 has been presented.

$$NH_2Cl + H_2O + C^* \rightarrow NH_4^+ + Cl^- + C^*O \quad (1)$$

$$2\ NH_2Cl + C^*O + 2\ H_2O \rightarrow N_2 + 2\ H_3O^+ + 2\ Cl^- + C^* \quad (2)$$

Removal of monochloramine and the type of reaction product formed by the degradation of monochloramine in GAC filters is highly relevant for the practical application of GAC in the treatment of swimming pool water. If only the reaction according to Equation 1 was taking place, then, during a full cycle of swimming pool water through the treatment system and back to the pool, only little effect would be achievable, as the re-chlorination of the treated water would again produce mono-, di- and trichloramine. Consequently, the application of GAC with a high N_2 yield is crucial to keep the concentration of inorganic chloramines and NDMA in the pool water at a constant, limited concentration.

Studies on the selective conversion of monochloramine to N_2 by activated carbon are scarce. There are only a few studies that have dealt with the importance of the chemical properties of the activated carbon surface for the N_2 yield. Fairey at al. (2007) concluded that the N_2 yield of the monochloramine–GAC reaction did not significantly differ among a set of five commercial GACs they had investigated. They concluded that the chemical characteristics of the individual GACs are irrelevant with respect to the N_2 yield. However, the observed N_2 yields ranged from 23 to 40% and only the low accuracy of the detection method prevented them from being able to significantly distinguish between the N_2 yields of the GACs investigated (Fairey at al., 2007).

Previous findings indicated that the rate of N_2 production correlates with the amount of oxide groups present at the GAC surface (see Equation 2). In this context, it is not known whether additional surface oxides are formed by the reaction of GACs with free chlorine (Equation 3) (Snoeyink et al., 1974; Suidan et al., 1977a; Suidan et al., 1977b; Suidan et al., 1977c) that is typically present besides chloramines in pool water and that affects monochloramine conversion to N_2.

$$C^* + HOCl + H_2O \rightarrow C^*O + H_3O^+ + Cl^- \quad (3)$$

Results from previous studies suggest that trace element constituents may favour monochloramine conversion to N_2. Various carbonaceous raw materials have been used to prepare activated carbons with different concentrations of heteroatoms and trace element compositions (Tsai and Chang, 1994; Sun and Webley, 2010; Sevilla et al., 2011; Wang et al., 2014). Among these, iron, lead and copper were found to catalyse the process of monochloramine decay (Vikesland and Valentine, 2002; Zhang et al., 2002; Edwards and Dudi, 2004; Switzer et al., 2006; Fu et al., 2009). Copper attracted particular interest because it favours disproportionation of monochloramine to form dichloramine (Fu et al., 2009) that in turn reacts with activated carbon to form N_2 according to Equation 4 (Bauer and Snoeyink, 1973; Scaramelli and Digiano, 1977).

$$2\ NHCl_2 + 5\ H_2O + C^* \rightarrow N_2 + 4\ H_3O^+ + 4\ Cl^- + C^*O \quad (4)$$

Consequently the primary objectives of this study were to understand the impact of chemical GAC properties such as the concentration of oxygen surface groups, elemental composition and traces of noble and transition metals on the yield of N_2 from the reduction of monochloramine at four different GACs available commercially. To ensure sufficient accuracy and practical relevance as well, long-term fixed-bed

141 experiments were carried out to determine reaction rate constants and yields under
142 conditions that are typical for swimming pool water. To test the correlation of
143 chemical carbon properties on rates and yields, acidic oxygen functionalities of the
144 used GACs, namely phenols, lactonic groups and carboxyl groups; the content of
145 noble and transition metals such as Pd, Rh, Mn, Co, Cu, Fe and Ni; and the
146 elemental composition of the carbons with respect to C, N, H and S were to be
147 analysed. Finally, in order to understand if and to what extent GAC treatment with
148 GACs that comprise a high N_2 yield could mitigate the concentration of chloramines
149 and NDMA in swimming pool systems, model calculations combining pool hydraulics
150 with the formation and abatement of inorganic chloramines and NDMA as well as
151 chloramine transformations in GAC filters were to be done.

2 Materials and Methods

2.1 Experimental determination of the carbon reactivity, NH_4^+ yield and N_2 yield

Many previous studies showed that the reduction of monochloramine in a fixed GAC bed can be described in sufficient detail using first order reaction kinetics (Skibinski et al., 2018; Kim, 1977; Scaramelli and Digiano, 1977; Kim and Snoeyink, 1980). Thus, for a GAC bed fed with a monochloramine solution with the inflow concentration $c_{bed,in}$ and the outflow concentration $c_{bed,out}$, the empty bed contact time (t_{EBCT}) is given by V_{bed}/Q_{bed}, where V_{bed} and Q_{bed} are the bed volume and the volumetric flow rate, and the apparent first order reaction rate constant k_{app} is obtained according to

$$k_{app} = \frac{1}{t_{EBCT}} \cdot \ln\left(\frac{c_{bed,in}}{c_{bed,out}}\right) \quad (5)$$

The procedure for determining k_{app} in fixed-bed column experiments under fully controlled conditions has been described previously by the authors (Skibinski et al., 2018). In brief, a laboratory-scale fixed-bed column with known bed volume (V_{bed}) and diameter (d_{bed}) was continuously fed, at a constant flow rate (Q_{bed}), with a monochloramine solution that was prepared from deionised water from a rapidly stirred double-walled glass tank with feedback-controlled pH and temperature. The effluent of the fixed-bed column was fed back into the glass tank. Monochloramine and free chlorine concentrations in the tank of the fixed-bed reactor (FBR) system were continuously measured using a membrane-covered amperometric 2-electrode total chlorine sensor (CTE-1 DMT, Prominent, Germany) that was calibrated daily using the photometric DPD method (DIN EN ISO 7393-2, 2000).

The concentration of monochloramine in the tank ($c_{bed,in}$) was kept constant during each experiment by feedback-controlled dosing (Q_{st}) of a highly concentrated monochloramine stock solution of 1.5 g L^{-1} (as Cl_2) (c_{st}). The outflow concentration of monochloramine $c_{bed,out}$ from the laboratory-scale fixed-bed column was indirectly calculated as described elsewhere (Skibinski et al., 2018). Identical repeated validation experiments conducted with the same system showed previously that the repeatability standard deviation of k_{app}, a measure that describes the precision of the experimental test method, was ±0.006 s^{-1} (Skibinski et al., 2018).

Fixed-bed column experiments were conducted under conditions that are typical for swimming pool water treatment. Experiments were run over several hours until stationary conditions of GAC reactivity were reached (Scaramelli and Digiano, 1977). Table 1 summarizes the operation conditions of the laboratory-scale fixed-bed column experiments.

As given by Equation 1 and 2, oxidation of GACs by monochloramine leads to the formation of oxygen surface groups, which in turn determine the yields of N_2 and ammonia of the monochloramine-GAC reaction. The rather short contact time in the column (2.88 s) was chosen to assure a homogeneous and thus, representative, oxidations state of the GAC bed across the columns bed depth. Further, previous studies showed that the time needed until k_{app} reached stationary conditions was very low for the small bed volume used in this study (32 mL) (Skibinski et al., 2018).

195 Table 1: Operation conditions of the laboratory-scale plant.

196 According to Equation 1 and Equation 2, monochloramine is converted in the filter
197 column forming NH_4^+ and N_2. The percentage of both reactions related to the overall
198 monochloramine conversion was determined by analysing the specific cumulative
199 amount of ammonium formed per g of GAC ($N_{NH4+}(t)$) since the beginning of an
200 experiment until time t per specific cumulative amount of monochloramine converted
201 per g of GAC in the filter column ($N_{MCA}(t)$) until time t. The average NH_4^+ yield
202 ($y_{NH4+}(t)$) at time t since the beginning of an experiment (Equation 6) was then
203 calculated from the slope of the linear regression between $N_{NH4+}(t)$ and $N_{MCA}(t)$.

$$y_{NH4+}(t)=\frac{N_{NH4+}(t)}{N_{MCA}(t)} \quad (6)$$

204 $N_{MCA}(t)$ was obtained as the integral of Q_{st} by c_{st} and by the differential reaction time
205 dt. Since ammonium was accumulating in the tank during an experiment, $N_{NH4+}(t)$
206 was obtained as the product of the concentration of ammonium in the tank after a
207 certain reaction time t and the total volume of water present in the laboratory-scale
208 plant. The photometric DPD method (DIN EN ISO 7393-2, 2000) was used to confirm
209 the absence of free chlorine in the monochloramine solution in the tank of the FBR
210 system over the run time of the experiments. This was of particular importance
211 because depletion of NH_4^+ formed in the filter column by chlorination reactions could
212 be neglected.

213 The N_2 yield ($y_{N2}(t)$) was determined indirectly as given in Equation 7, assuming that
214 NH_4^+ and N_2 were the only nitrogenous reaction products present in the tank (Bauer
215 and Snoeyink, 1973; Fairey et al., 2007).

$$y_{N2}(t) = 1 - y_{NH4+} \quad (7)$$

2.2 Preparation of the monochloramine and HOCl stock solution

All solutions were prepared using ultrapure water (Millipore direct Q UV3 water purification system, Merck Millipore, Germany). Monochloramine stock solutions used in the fixed-bed column experiments were prepared as described in detail previously (Skibinski et al., 2018) by slowly adding a HOCl solution (0.032 mol L^{-1}) to an ammonia stock solution (0.098 mol L^{-1}) to reach a final molar ratio of chlorine to ammonia of 1.00:1.03 at pH 10 under stirring (Aoki, 1989). Monochloramine and HOCl stock solutions were stored protected from light at 4°C before use.

2.3 Granular activated carbons

Four commercially available GACs, Hydraffin 30N from Donau Carbon GmbH (30N), Centaur from Chemviron Carbon GmbH (Centaur), Silcarbon K-835 from Silcarbon Aktivkohle GmbH (K835) and Saratec 100058 from Bluecher GmbH (100058) were used in this study. The raw materials were anthracite coal (30N), coconut shells (K835), bituminous coal (Centaur) and non-porous polymer-based spheres (100058). According to the specifications provided by the manufacturers, the GACs had been produced by initial carbonisation of the different raw materials at low temperatures, followed by physical activation with steam (30N, 100058) (Fichtner, 2010; Branton et al., 2011; Böhringer et al., 2011), steam and carbon dioxide (K835) (Raave et al., 2014) or impregnation with urea and subsequent heating (Centaur) (Matviya and Hayden, 1994; Hayden, 1995). The mean grain diameters of the used carbons (d_{60}) were as follows: 1.57 mm (K835), 1.51 mm (30N), 1.27 mm (Centaur) and 0.51 mm (100058). The respective grain size distributions are given elsewhere (Skibinski et

al., 2018). Before use, the fresh GACs were treated by: (i) soaking in ultrapure water, (ii) evacuating the soaked suspension of GAC and (iii) washing and decantation as described previously by Skibinski et al. (2018).

2.4 Altered granular activated carbons

As the reaction to N_2 according to Equation 2 requires the presence of surface oxides, it is to be expected that an increased concentration of surface oxides on the activated carbon will increase the reaction rate according to Equation 2 and the N_2 yield. Therefore, in order to determine the impact of surface oxide concentration on the N_2 yield of the monochloramine–GAC reaction, fixed-bed column experiments were performed with GACs that had been pre-treated with HOCl according to Equation 3. The laboratory-scale fixed-bed column was operated as described in Section 2.1 but instead of using a solution of monochloramine, a highly concentrated HOCl stock solution (4.5 mg L^{-1} (as Cl_2)) was added to the glass tank. Experiments with HOCl were run until ~2.2 mmol g_{GAC}^{-1} of HOCl (as Cl_2) reacted in the laboratory-scale GAC filter. The GACs remained in the filter column after HOCl treatment. Thereafter, the fixed-bed column was operated with a solution of monochloramine to determine the N_2 yield of the monochloramine–GAC reaction.

2.5 Analytical quantification of monochloramine, free chlorine and ammonium

The concentration of the monochloramine stock solutions was determined spectrophotometrically on a daily basis taking into account the overlapping absorbance peaks of monochloramine and dichloramine ($NHCl_2$) at 245 nm and 295 nm ($\varepsilon_{NH2Cl,\ 245\ nm}$ = 445 L mol^{-1} cm^{-1}, $\varepsilon_{NHCl2,\ 245\ nm}$ = 208 L mol^{-1} cm^{-1},

263 $\varepsilon_{NH2Cl,\ 295\ nm}$ = 14 L mol^{-1} cm^{-1}, $\varepsilon_{NHCl2,\ 295\ nm}$ = 267 L mol^{-1} cm^{-1} (Schreiber and Mitch,
264 2005)) (results not shown).

265 Spectrophotometric measurements at 360 nm confirmed the absence of
266 trichloramine (NCl_3) in the monochloramine stock solution
267 ($\varepsilon_{NCl3,\ 360\ nm}$ = 126 L mol^{-1} cm^{-1}) (Valentine et al., 1986; Schurter et al., 1995).

268 The HOCl stock solutions were standardised spectrophotometrically at pH 10 as the
269 OCl^- ion using a molar absorption coefficient at 294 nm ($\varepsilon_{OCl-,\ 294nm}$) of
270 348 L mol^{-1} cm^{-1} (Hand and Margerum, 1983). A Unicam UV2-200 UV/VIS
271 spectrophotometer was used for the absorbance measurements.

272 For quantification of ammonium (NH_4^+), samples were taken from the tank and
273 analysed by size exclusion chromatography with organic carbon and organic nitrogen
274 detection (LC-OCD-OND) as described elsewhere (Huber et al., 2011a). It should be
275 noted that although the LC-OCD-OND was designed for organic nitrogen detection, it
276 is also capable of quantifying inorganic nitrogen compounds such as ammonium
277 (Huber et al., 2011b). Samples were stored in headspace-free vials with screw caps
278 (25 mL) at ~4°C until analysis with LC-OCD-OND that followed within 12 h after
279 sampling. The limit of detection for ammonium is assumed to be equal to that of urea
280 (1 ppb) previously determined by using the LC-OCD-OND method (Huber et al.,
281 2011b). Finally, LC-OCD-OND analysis confirmed that no other nitrogen containing
282 substances were present in the water samples taken from the tank.

283 **2.6 Chemical characterisation of the granular activated carbons**

284 Boehm titration

Boehm titration (Boehm, 1966), recently standardised (Goertzen et al., 2010; Oickle et al., 2010), was used to quantify the oxygen groups present on the GAC surface. This method allows distinguishing oxygen groups by their different acidity, in particular phenols, lactonic groups and carboxyl groups. For analysis, the fresh and altered GACs were dried over a period of 24 h at 70°C to avoid volatile surface oxides being removed by drying (Snoeyink et al., 1974). Then, 1.5 g of the carbon was suspended in 50 mL solutions of either 0.05 mol L^{-1} $NaHCO_3$, Na_2CO_3 or NaOH. After shaking the suspensions at 150 rpm for 24 h, the samples were filtered using 0.45 µm polycarbonate track etch membrane filters (Sartorius AG, Germany). Aliquots (10 mL each) of the filtered $NaHCO_3$ and NaOH solutions were each acidified with 20 mL 0.05 mol L^{-1} HCl, and a 10 mL aliquot of the filtered $NaCO_3$ sample was acidified with 30 mL 0.05 mol L^{-1} HCl. CO_2 was stripped from the acidified samples by continuously sparkling with N_2 for 2 h. Finally, 0.05 mol L^{-1} NaOH was added drop-wise to the acidified samples under simultaneous sparkling with N_2, until pH 7 was reached. The volume of 0.05 mol L^{-1} NaOH needed to reach pH 7 was denoted as V_{NaOH} and was determined in triplicate for each batch experiment. The amount of carbon surface functionalities in terms of phenols, lactonic groups and carboxyl groups were calculated based on V_{NaOH} as described elsewhere (Goertzen et al., 2010; Oickle et al., 2010).

Zeta potential

To further elucidate the acidic character of the GACs, the zeta (ζ) potential of the fresh GACs was measured from their electrophoretic mobility (Sze et al., 2003) using a Zetasizer Nano ZS equipped with an MPT-2 autotitrator (Malvern Instruments, Worcestershire, UK). For zeta analysis, the GACs were ground to powdered carbon using a ball mill (PM100, Retsch, Germany). A suspension of the powdered carbon was prepared in 0.01 mol L^{-1} KCl solution. After a settling time of ~24 h, the supernatant of the suspension was used for analysis. Zeta potentials were analysed at different pH as described by Strelko et al. (2002). Adjustment of the pH was performed by dosing solutions with either 0.1 mol L^{-1} HCl or 0.1 mol L^{-1} NaOH. Zeta potentials are given as the average of three replicates. The isoelectric point of the GACs is taken to be the pH at which the surface exhibits a neutral net zeta potential.

Trace metal content

The concentration of two groups of elements widely used as catalysts (e.g., noble metals (Pd, Rh) and transition metals (Mn, Co, Cu, Fe and Ni) (Goifman et al., 2006; Liu et al., 2013)) in the fresh GACs were analysed by inductively coupled plasma atomic emission mass spectroscopy (ICP-MS) using a PQexCell instrument (Thermo Fisher Scientific Inc., USA) according to the German standard DIN-EN-ISO-17294-2 (2004). Prior to ICP-MS analysis, powdered samples of the dried fresh GACs were digested for 30 min in a closed PTFE vessel at 180°C by microwaves (MARS 5 CEM Corp., United States). For digestion, 0.5 g of ground carbon was suspended in a mixture of 5 mL concentrated nitric acid (HNO_3), 1 mL H_2O_2 (30 %) and 5 mL ultrapure water. Digested samples were filtered by a 0.45 µm polycarbonate track etch membrane filter (Sartorius AG, Germany) and subsequently diluted with ultrapure water to 50 mL. Diluted samples were then analysed by ICP-MS.

Concentrations of trace metals are reported as the mean value of two replicates. The limits of detection for the method were calculated as the threefold standard deviation of blank samples. Blank samples were prepared according to the above-described routine but without the carbon sample.

Elemental analysis

Analysis of the carbon, hydrogen and nitrogen content of the GACs was performed using a CHN element analyser (Vario EL, Elementar Analysesystem GmbH). The sulphur content of the GACs was analysed according to the German standard DIN 51724-3 (2012) using an Eltra CS 580 analyser. The following amounts of powdered GAC samples were used: 5 – 7 mg (C, N, H) and 100 – 150 mg (S). The C, N, H and S content of the GACs is given as the mean of two replicates. The limits of detection were 0.007 g g_{GAC}^{-1} (C), 0.017 g g_{GAC}^{-1} (N), 0.003 g g_{GAC}^{-1} (H) and <0.05 g g_{GAC}^{-1} (S).

2.7 Statistical analysis

Student's t-tests were used to test for a difference in NH_4^+ yields between the GACs investigated. The null hypothesis that states that no differences were observed was rejected for a probability of <0.05.

To determine if any of the chemical carbon properties could function as an indicator for the apparent N_2 yield, Pearson correlation coefficients were calculated for the linear correlation between the trace element concentrations of the GACs and the N_2 yield. Only linear correlations with a coefficient > 0.9 have been further considered for descriptive analysis. Therefore, an assessment of the graphical visualisation of the dependency of the N_2 yield on the corresponding concentration of surface oxygen groups or trace elements was carried out.

354 Due to the low number of tested carbons (n = 4), a determination of the significance
355 of the linear correlations as well as a multivariate analysis on the synergetic effect of
356 different chemical carbon properties on the N_2 yield were not carried out.

357 If not mentioned otherwise, errors are given as 95 % confidence interval, calculated
358 from the standard deviation, number of observations and the t-distribution.

3 Results and Discussion

3.1 Carbon reactivity and reaction products

In Figure 1(A-D), the specific amount of NH_4^+ produced per g of GAC as well as the apparent reaction rate constant k_{app} are plotted against the amount of monochloramine degraded when using filter beds of the 30N, K835, Centaur and 100058 carbons. In agreement with previous findings, k_{app} initially decreased until quasi stationary conditions were reached (Fairey et al., 2007), which was after 0.75 to 1.25 mmol of monochloramine had reacted per g of GAC (equivalent to 75 – 125 h of filter run time). The decrease in reactivity has previously been explained by an increase in diffusional resistance with on-going reaction time (Skibinski et al., 2018). In brief, it is assumed that the monochloramine-GAC reaction that starts first at the outer surface of the GAC grains, and the reaction front then moves towards the centre of the grains with on-going reaction time leaving behind reacted carbon sites. The fact that k_{app} did not decrease until zero when stationary conditions were reached could be explained by oxygen groups that continuously evolve from the surface as CO or CO_2, thus providing new free active sites (Snoeyink et al., 1974). The reaction rate constants k_{app} at stationary conditions were found to be 0.015 s^{-1} (100058), 0.016 s^{-1} (30N), 0.018 s^{-1} (K835) and 0.024 s^{-1} (Centaur). The unusual course of k_{app} for the 100058 carbon has been discussed previously and was explained by a shift in the reaction-controlling mechanism due to the inhomogeneous pore size distribution of the 100058 carbon (Skibinski et al., 2018).

The NH_4^+ yields of the respective GACs were derived from the slope of the plot of the cumulative amount of NH_4^+ produced versus the cumulative amount of monochloramine removed in the GAC bed (see Figure 1(A-D)). The linear correlation for all GACs indicates that the NH_4^+ yield did not change during the course of the

reaction. The coefficient of determination (r^2) for linear fitting ranged from 0.993 to 0.999, indicating that the linear regression provides an adequate fit to the experimental data. The NH_4^+ yields for the GACs were found as follows: 78.7±3.6% (K835) < 88.4±2.30% (100058) < 95.8±2.2% (Centaur) < 99.5±4.2% (30N). To assess the reliability of the measured NH_4^+ yields, experiments with the K835 carbon were repeated three times (data not shown). Hypothesis testing ($p<0.05$) showed no significant differences in the NH_4^+ yield among the three repetitions, indicating a satisfactory reproducibility. For the Centaur GAC, Fairey et al. (2007) reported a NH_4^+ yield of 69±11 %, which is far lower than the 95.8±2.2 % ($p < 0.001$) found in the present study. As will be discussed below in Section 3.4, this is most probably due to strong variations in the different batches of that GAC.

The N_2 yields, calculated as described in Section 2.1, were as follows: 0.5±4.7% (30N) < 4.2±3.0% (Centaur) < 11.6±3.1% (100058) < 21.3±4.1% (K835). Slightly higher N_2 yields of other GACs were reported in previous fixed-bed column studies (42% (Scaramelli and Digiano, 1977), 23 to 40% (Fairey et al., 2007) and 27.3% (Kim, 1977)). Contrary to the findings of Fairey et al. (2007), hypothesis testing ($p<0.05$) in this study showed that the differences in N_2 yields among the tested GACs were significant. Table A.1 in the supporting material (SM) lists other processes that potentially could have an effect on the observed N_2 yield of the monochloramine–GAC reaction but were determined to be negligible.

Figure 1: Reaction rate constant and specific amount of NH_4^+ produced per g GAC versus the specific amount of monochloramine removed per g of GAC for the 30N (A), K835 (B), Centaur (C) and 100058 (D) GACs. Error bars for k_{app} represent the standard deviation (n = 20). Solid lines represent the linear least-squares best fit of the correlation between monochloramine removed and NH_4^+ produced. Dashed lines represent the corresponding 95% confidence band of the fitted regression. The NH_4^+ yields from monochloramine removal were derived from the slope of the linear regressions. Errors of the NH_4^+ yield represent the error of the slope of the linear correlation.

3.2 Formation of surface oxygen groups

3.2.1 Characterisation of fresh GACs

Acidic oxygen groups

The amounts of acidic oxygen groups present on the surface of the GACs as determined by Boehm titration are shown in Table 2. Values are given for the fresh and altered GACs as analysed at the end of the FBR experiments. The fresh GACs contained total acidic oxidised functionalities in a concentration range from 1728 to 1926 µmol g_{GAC}^{-1}. The majority of acidic oxygen groups were present as carboxylic groups, whereas only small amounts of lactonic and phenolic groups were present. This composition is typical for activated carbons (Cagnon et al., 2005; Kalijadis et al., 2011; Allwar, 2012).

ζ potential

Figure 2 shows the ζ potential of the fresh 100058, K835, 30N and Centaur GACs. For the 100058, K835 and Centaur GACs, the ζ potential decreased steeply with increasing pH until it remained constant above a pH of ~8 to 10. The net negative charge in this pH range can be explained by the dissociation of carboxylic groups, which occurs between pH 2 to 6 for activated carbons (Strelko et al., 2002; Chingombe et al., 2005). Even though the fresh 30N carbon had the same level of carboxyl groups compared to the other fresh carbons (see Table 2), its change in zeta potential between pH 2 and 6 was comparatively low. This could be explained by a more homogeneous distribution of carboxylic groups between internal and external particle surfaces for the 30N carbon (Memendez et al., 1995). For the K835, 100058 and Centaur carbon, a significant amount of carboxylic groups is assumed to be located at the external surface of the carbon grains, thus, having a more pronounced effect on the electrophoretic mobility (i.e. zeta potential) compared to the 30N carbon.

Further, the fresh 30N carbon has a higher isoelectric point (pH_{IEP}) of ~7.2 when compared to the other fresh GACs (pH_{IEP} = ~2). As all carbons comprised almost the same amount of total acidic groups, this indicates that a significantly higher amount of groups with basic properties imparts the surface of the 30N carbon (Memendez et al., 1995).

Due to the high amount of carboxylic functionalities suggested by the change in ζ potential with pH, the main focus for further characterisation was on acidic functionalities rather than on basic groups that were not further quantified. It should be noted here that the activated carbon grains had been ground prior to the determination of the zeta potential, which may have altered their surface chemical properties.

Figure 2: Zeta potentials of the fresh 100058, 30N, K835 and Centaur GACs at different pH. Error bars represent the standard deviation of three repeated experiments.

3.2.2 Characterisation of altered GACs

The amounts of total acidic surface groups formed over the course of the FBR experiments (Table 2) were as follows: 240 µmol g_{GAC}^{-1} (Centaur) < 282 µmol g_{GAC}^{-1} (30N) < 364 µmol g_{GAC}^{-1} (100058) < 368 µmol g_{GAC}^{-1} (K835). With the increase in the concentration of total acidic groups, a slight change in the composition of specific oxygen groups (i.e. carboxylic, phenolic and lactonic) revealed. The percentage of phenolic groups of the tested GACs increased by ~3%, whereas the percentage of carboxylic groups decreased by ~7% (mean value of all GACs). Hypothesis testing ($p<0.05$) showed that the differences in the amounts of lactonic groups were not significant.

The highly disorganized structure of activated carbons consists of amorphous carbon and crystalline, graphitic microstructures. The edges of these microstructures consist of unsaturated C-C bonds (Xiang et al. 2016) and heteroatoms, usually bonded to these sites, could give rise to the formation of oxygen surface groups by wet oxidation (e.g. by HOCl (Menendez-Diaz and Martin-Gullon 2006) or monochloramine (Fairey et al. 2006)). Further, previous studies suggest that the formation of oxygen functionalities, such as carboxylic functions, could imply the cleavage of an aromatic ring by strong oxidants (Perrard et al. 2012).

Snoeyink et al. (1974) previously reported an increase in the total acidic surface groups of ~1.000 µmol g_{GAC}^{-1} when oxidising GACs with hypochlorous acid (HOCl). The higher concentration of surface oxides found by Snoeyink et al. (1974) compared to those found in this study can be explained by the higher oxidation potential of HOCl than monochloramine.

A correlation analysis was conducted for the amount of oxygen groups (i.e. carboxylic, phenolic and lactonic) present on the surface of the fresh and oxidised GACs and the corresponding N_2 yield. All correlation coefficients were < 0.9.

Further, a correlation analysis was conducted for the amounts of oxygen groups formed on the surface of the oxidised GACs over the course of the FBR experiments (Section 3.1) and the corresponding N_2 yield. The correlation coefficients were 0.94 for the high amount of carboxylic groups formed and -0.94 for the low amount of phenols formed. Since long term experiments revealed that the N_2 yield did not change with on-going oxidation by monochloramine (see Figure 1), these findings were determined to be negligible.

In summary, it can be concluded that GAC surface oxidation by monochloramine leads to an increase in the amount of oxygen surface groups accompanied by a minor change in the composition of acidic oxygen functionalities. These findings give evidence that a proportion of monochloramine reacts at carbon surfaces according to Equation 1. However, the N_2 yield of the monochloramine–GAC reaction was unaffected by the amount or type of oxygen groups formed at the carbon surface with on-going reaction time. These findings contradict the mechanism indicated by Equation 2, raising doubt that monochloramine transformation at surface oxides is a feasible explanation for the observed transformation of monochloramine to N_2. An

499 important reason for the absence of the expected change in N_2 yield could be the
500 comparably low amount of total acidic oxide groups formed over the course of the
501 reaction (240 µmol g_{GAC}^{-1} - 368 µmol g_{GAC}^{-1}).

502 Table 2: Concentration of acidic oxygen groups on the surface of the fresh and
503 altered GACs and correlation analysis for the dependence of N_2 yield
504 on the acidic oxygen surface groups.

505 **3.3 Impact of HOCl pre-treatment on the N_2 yield**

506 In order to clarify, if the concentration of surface oxides affects the observable
507 N_2 yield, the fresh K835 and Centaur carbon were pre-treated with HOCl prior to the
508 determination of the N_2 and NH_4^+ yield of the monochloramine–GAC reaction.

509 Figure B.1 (SM) presents the reactivity of the K835 and Centaur carbon for HOCl
510 removal with increasing reaction time. As for monochloramine removal, the carbon
511 reactivity for HOCl removal decreased until k_{app} reached an almost constant value.

512 The decrease in reactivity for monochloramine (see Figure 1) has been assigned to
513 an increase in diffusional resistance with on-going reaction time (see Section 3.1).
514 Assuming that the same process applies to the reaction of HOCl at GAC grains, it
515 could be assumed that the reaction of HOCl starts at the outer surface of the GAC
516 grains and the reaction front then moves towards the centre of the grains with on-
517 going reaction time leaving behind reacted carbon sites. The stationary first-order
518 reaction rate constants for HOCl removal were higher than those for monochloramine
519 removal by a factor of ~3.

520 Figure 3(A-B) shows the reaction rate constant k_{app} and the amount of NH_4^+
521 produced for the monochloramine–GAC reaction after HOCl pre-treatment. The

apparent reaction rate constant k_{app} for monochloramine removal did not change during the GAC filtration after HOCl pre-treatment. This could be explained by the fact that the external and internal surface of the carbon has already been oxidized by HOCl.

Following Equation 2, it is hypothesised that the formation of oxygen groups at the GAC surface caused by HOCl pre-treatment (Snoeyink et al., 1974) enhances the conversion of monochloramine to N_2 as more surface oxides are formed. It has been shown previously that oxidation by HOCl also leads to the formation of mostly the same types of surface oxides (carboxylic and hydroxylic groups) (Hassan and Yasin, 2015) compared to those found in this study formed from oxidation by monochloramine.

However, compared to the NH_4^+ yield observed before the GACs were treated with HOCl (see Figure 1(B-C)), the differences were -0.5% (K835) and -5.8% (Centaur). Taking into account the precision of the method, as expressed by the standard deviation observed, these differences were considered to be not significant ($p<0.05$).

Since no change in NH_4^+ yield (and N_2 yield) occurred after HOCl treatment, the impact of acidic oxygen functionalities present at the carbon surfaces on monochloramine conversion to N_2 was determined to be negligible. These findings contradict the reaction mechanism reported previously (Equation 2) and indicate that the concentration of surface oxides only partly determines the N_2 yield of monochloramine conversion in GAC filters. An alternative mechanism that could be responsible for the observed N_2 yields is presented in Section 3.4.

Figure 3: Reaction rate constant k_{app} and specific amount of NH_4^+ produced per g GAC plotted against the specific amount of monochloramine degraded per g GAC for the K835 (A) and Centaur (B) GACs after HOCl pre-treatment. Error bars for k_{app} represent the standard deviation (n = 20). Solid lines represent the linear least-squares best fit of the correlation between monochloramine removed and NH_4^+ produced. Dashed lines represent the corresponding 95% confidence band of the fitted regression. Errors in the NH_4^+ yield represent the errors in the slope of the linear correlation. Interruptions in the k_{app} curve were caused by imperfect data acquisition.

3.4 Impact of trace elements on the N_2 yield

The elemental analysis of the fresh GACs and the results of the correlation analysis for the dependency of the N_2 yield on the elemental composition of the GACs are presented in Table 3. The elemental analysis showed that the Centaur carbon comprised the highest amount of nitrogen and the second highest amount of sulphur among the GACs investigated. Previous studies suggested an increased catalytic activity for carbons with a high nitrogen content (e.g., for oxygen reduction reactions (Zhang et al., 2014a; Zhang et al., 2014b)) or presence of thiol groups (e.g. monochloramine removal (Jacangelo et al., 1987)). The high nitrogen content of the Centaur GAC is explained by the manufacturing method that included impregnation of the carbonised raw material with urea prior to the activation step (Hayden, 1995; Matviya and Hayden, 1994). However, correlation analysis showed that correlation coefficients for the correlation between the concentration of heteroatoms in the GACs and the corresponding N_2 yield of the monochloramine–GAC reaction were < 0.55 (Table 3).

569 The content of trace metals found in the considered GACs was typical for activated
570 carbons prepared from natural raw products (Tsai and Chang, 1994). It has been
571 shown in previous studies that metals such as Fe, Pd or Cu can favour
572 monochloramine conversion to either NH_4^+ or N_2 (Vikesland and Valentine, 2002;
573 Edwards and Dudi, 2004; Switzer et al., 2006; Fu et al., 2009). The correlation
574 coefficients are given in Table 3. Except for copper, the correlation coefficients were
575 < 0.9. For copper, however, r = 0.95. The analysis of the graphical visualisation of the
576 dependency of the N_2 yield on the corresponding concentration of copper (Figure not
577 shown) showed an even distribution of the data points, indicating that no outlier
578 caused the high r. Thus, for copper the hypothesis of a correlation between the
579 copper content of a GAC and the N_2 yield was accepted. Further, the graphical
580 visualisation revealed that transformation of monochloramine to N_2 increased only
581 when a certain minimal copper concentration was present at the carbon surface.

582 Previous batch studies that support this hypothesis showed that copper catalyses
583 monochloramine decay by direct catalysis of Cu(II) and indirect catalysis of the active
584 radical intermediates formed. In case of direct catalysis, which was found to be the
585 primary reaction path (Fu et al., 2009), monochloramine is degraded to dichloramine
586 (Equations 8 and 9):

$$Cu^{2+} + NH_2Cl \rightarrow [Cu^{II}NH_2Cl]^{2+} \textit{ (complex)} \quad (8)$$

$$[Cu^{II}NH_2Cl]^{2+} + NH_2Cl \rightarrow NHCl_2 + NH_3 + Cu^{2+} \quad (9)$$

587 Assuming the same process occurs in GAC, dichloramine would be further converted
588 at active carbon surface sites to N_2 according to Equation 4 (Kim et al., 1978).
589 Further products of the reaction system of NH_2Cl and Cu(II) are NHCl• and NH_2•
590 radicals (Fu et al., 2009). Self-merging reactions between the NH_2• radicals lead to
591 the formation of N_2 as an end product as well (Fu et al., 2009). Both direct and

indirect catalysis of the decay of monochloramine by Cu(II) provide a feasible explanation for the high monochloramine conversion to N_2 found for GACs with a high Cu content. It further has to be acknowledged that the proposed mechanism for monochloramine transformation via copper catalysis only includes the proportion of monochloramine that is transformed to N_2. Another proportion of monochloramine still reacts with active sites on the carbon surface (see Equation 1) forming oxygen groups over the course of reaction, as it has been in the experiments conducted in the present study (see Table 2). It is subject to further research to verify the proposed mechanism that explains the importance of copper on carbon surfaces for monochloramine transformation and establish an overall reaction scheme for monochloramine transformation, including monochloramine reactions with copper and the carbon material.

It should be noted here that, according to data in the literature, the copper content varies significantly among different batches of the Centaur carbon (e.g., 24.16 µg g^{-1}_{GAC} (Gardner et al., 2002) and 12.2±2.0 µg g^{-1}_{GAC} (this study)). Such differences may cause the different conversion of monochloramine to NH_4^+ found in this study and in previous measurements (Fairey et al., 2007) (see Section 3.1).

Table 3: Elemental analysis of the tested GACs and correlation analysis for the dependency of the N_2 yield on the elemental composition.

4 Predicting concentrations of chloramines and NDMA in pool water depending on the carbon type used in the GAC filter

4.1 The numerical swimming pool model

In order to determine the effect of the carbon type (apparent rate constant and N_2 yield) used in a GAC filter on concentrations inorganic chloramine and NDMA in real swimming pool systems, a simplified numerical model of a swimming pool was set up using the software AQUASIM (Reichert, 1994). The numerical pool model is based on the simplified hydraulic approach by Cloteaux et al. (2013) and consists of a pool basin, a fresh water inlet and a water recirculation with GAC filter and its chloramine transformation reactions (see Figure C.1 (SM)). Further, loading with ammonium and urea form the bathers, chlorine reactions with ammonia (Jafvert and Valentine, 1992) and urea (Blatchley and Cheng, 2010; Gérardin et al., 2015) as well as NDMA formation by the reaction of chloramines with DMA (Schreiber and Mitch, 2006) were taken into account in the model.

The first-order decomposition rate constants k_{app} determined in the experiments conducted in the present study (see Section 3.1) were used in the model simulation. The first-order approach has previously been found to be applicable to typical bed depth used in real-scale GAC filters (Scaramelli and Digiano, 1977, Becker et al. 1990) and has been found to be valid for a wide range of temperatures, flow velocities and inflow-concentrations (Skibinski et al., 2018), that also cover those of the numerical swimming pool model. As the temperature of the experimental determination of k_{app} in this study was the same as that of the numerical swimming pool model, a temperature correction of k_{app}, as proposed previously by the authors (e.g. via the Arrhenius equation, Skibinski et al., 2018), was not applied. As yields of N_2 and ammonia revealed to be constant throughout a long time of operation and

with on-going oxidation of the GACs in the experiments conducted in the present study (Figure 1), the same constant yields of N_2 and ammonia for monochloramine transformation at GACs were used for the numerical swimming pool model.

A more detailed description of the numerical swimming pool model, its reactions and simulation runs performed, are given in Section C (SM).

4.2 Modeling results

Each simulation run was started with the pool system being filled with pure water that did not contain any of the respective reactants, intermediates or products. Simulations were performed at continuous bather loading until stationary concentrations of all the respective species in the pool were reached. Each single simulation run was performed with a certain GAC (i.e., a specific set of k_{app} and N_2 yield). Table D.1 (SM) summarizes the k_{app} values and N_2 yields used.

Figure 4 shows the simulated, relative monochloramine concentration profiles ($c(z)/c_{bed,in}$) over the bed depth of the theoretical full-scale GAC filter using the k_{app} values of the four commercial GACs tested in this study. Equal profiles have been simulated for other GACs tested in previous studies (see Table D.1 (SM)) as well, but are not shown here. It revealed that monochloramine is only partially removed across the total bed depth of the GAC filters of 0.9 m. The relative monochloramine removal for the GACs tested in this study was the following: 80.6 % (100058) < 82.4% (30N) < 86.1% (K835) < 92.6 % (Centaur). The relative amounts of transformation products (N_2 and NH_4^+) formed over the bed depth of the GAC filters are shown in Figure E.1 (SM). The amount of monochloramine converted to N_2 across the GAC filter depends on the N_2 yield of the particular carbon rather than on the carbon reactivity, as expressed in the rate constant k_{app}.

660

661 Figure 4: Simulated normalised monochloramine concentrations over the bed
662 depth of a theoretical GAC filter (z_{bed} = 0.9 m) for the K835, 30N,
663 Centaur and 100058 GACs. Concentration profiles were calculated
664 according to Equation C.1 (SM) using a v_{eff} of 30 m h^{-1}. The reaction
665 rate constants used for calculation were those observed when
666 stationary conditions were reached (see Figure 1).

667 Figure 5 shows an example of the simulated time dependent concentration of
668 inorganic chloramines and NDMA in the pool for a system making use of GAC filters
669 of the K835 GAC and of 0.9 m depth. The time needed to reach stationary conditions
670 in the pool was ~2 h for inorganic chloramines and up to ~1000 h for NDMA. The fact
671 that the time needed to reach stationary chloramine concentrations in the pool was
672 lower than the hydraulic retention time of the pool (~3 h) could primarily be explained
673 by the high rate constants for chloramine formation (reaction 1, 3 and 11, Table C.2
674 (SM)) and consequently, the fast depletion of free available ammonium. Ammonium
675 concentrations in the numerical pool were very low (< 0.0018 mg L^{-1}), when
676 stationary conditions were reached. Previous studies found that ammonia itself is
677 typically not present in a chlorine treated pool (Wojtowicz, 2001), thus supporting
678 these findings. The time needed to reach stationary NDMA concentrations could
679 primarily be explained by the low rate constants for NDMA formation (reaction 27,
680 Table C.2 (SM)).

681 Modelled concentrations in the pool at steady-state were 0.17 mg L^{-1} (as Cl_2) (sum of
682 inorganic chloramines), 0.1 mg L^{-1} (as Cl_2) (monochloramine), 0.04 mg L^{-1} (as Cl_2)
683 (dichloramine), 0.03 mg L^{-1} (as Cl_2) (trichloramine) and 0.012 ng L^{-1} (NDMA). Mean

684 concentrations of chloramines and NDMA in full-scale pools with almost equal
685 concentrations of free chlorine (~0.5 mg L^{-1} (as Cl_2)) as determined over a period of 6
686 month were slightly higher: 0.23 mg L^{-1} (as Cl_2) (sum of inorganic chloramines),
687 0.17 mg L^{-1} (as Cl_2) (monochloramine), 0.05 mg L^{-1} (as Cl_2) (dichloramine),
688 0.01 mg L^{-1} (as Cl_2) (trichloramine) (Weaver et al., 2009) and 0.06 to 5.9 ng L^{-1}
689 (NDMA) (Jurado-Sanchez et al., 2010; Soltermann et al., 2012; Lee et al., 2013).
690 Since the frequency of bathers entering the full-scale pools over time was not given
691 by the authors, this data cannot be used to validate the numerical pool model.
692 However, it can be concluded that the overall magnitude of concentrations shows an
693 adequate similarity between modeled and full-scale results.

694

695 Figure 5: Evolution of simulated concentrations of mono-, di- and trichloramine
696 (A) and NDMA (B) in the simplified numerical pool model. As an
697 illustrative example, the carbon reactivity k_{app} and N_2 yield of the
698 carbon were chosen to be that of the K835 carbon (k_{app} = 0.0183 s^{-1},
699 N_2 yield = 21.3 %).

700 Figure 6 shows the effect of both, k_{app} and N_2 yield, on the stationary concentrations
701 of inorganic chloramines (sum of mono-, di- and trichloramine) and NDMA in the
702 basin of the simplified numerical pool model. Simulation results are displayed as the
703 relative reduction compared to the scenario without a GAC filter. For the purpose of
704 comparison, the removal performance of the GACs used in this study (30N, K835,
705 Centaur and 100058) and those considered in previous fixed-bed column studies
706 (Scaramelli and Digiano, 1977; Fairey et al., 2007; Kim, 1977) are displayed. Table
707 D.1 (SM) summarizes the k_{app} values and N_2 yields used. Among a variety of

considered GACs, the reductions relative to the scenario without a GAC filter ranged from 0.5 to 2.7% (inorganic chloramines) and from 1.7 to 4.5% (NDMA), depending on the GAC used. Thus, the model results confirm the initial hypothesis that conversion of monochloramine to N_2 in GAC filters sustainably reduces the concentrations of inorganic chloramines and NDMA in the basin of a pool system. Moreover, the results indicate that the reduction of chloramines and NDMA can be increased by a factor of ~2 if the tested GACs can be modified to comprise a N_2 yield of up to ~50%. By comparing the concentrations of chloramines and NDMA in the basin at the same N_2 yield but different k_{app}, it becomes clear that concentrations of chloramines and NDMA change only slightly for k_{app} higher than ~0.020 s^{-1}. This could be explained by the fact that almost all monochloramine is removed across the GAC filter for reaction rate constants >0.020 s^{-1}.

Figure 6: Impact of k_{app} and N_2 yield on stationary concentrations of inorganic chloramines and NDMA as simulated using the simplified numerical swimming pool model. Results are displayed as the normalised concentration reduction when related to the scenario without a GAC filter.

5 Summary and Conclusions

Using a fixed-bed reactor system, yields of monochloramine conversion by a chemical surface reaction to elemental nitrogen (N_2) in GAC beds were determined under conditions typical for swimming pool water treatment. N_2 yields ranged between 0.5±4.7% and 21.3±4.1% for the four GACs tested. No significant change in N_2 yield was found with on-going exposure of the GAC to monochloramine. Contrary to the N_2 yield, the apparent reaction rates for the removal of monochloramine in GAC beds initially decreased until quasi-stationary conditions were reached after 0.75 to 1.25 mmol $g_{GAC}^{-1}$of monochloramine had reacted. When quasi-stationary conditions had been reached, a total of 240 – 368 µmol g_{GAC}^{-1} of oxygen groups were formed by monochloramine oxidation, with carboxylic groups being the prevailing type. Contrary to previous assumptions, the N_2 yield did not correlate with the amount of oxygen groups present on the carbons surface. This was also true after intense pre-oxidation of the GACs with ~2.2 mmol g_{GAC}^{-1} (as Cl_2) of hypochlorous acid.

Correlation analysis between the trace elemental composition of the GACs and the N_2 yield indicates a linear dependency of the N_2 yield on the copper content of the GACs ($r = 0.95$). This can be explained by direct catalysis of the disproportionation of monochloramine by Cu(II), forming dichloramine. Assuming the same process takes place in GAC beds, dichloramine will be further converted at active carbon surface sites to N_2.

These findings still have to be verified in future experiments testing a higher number GACs with different amounts of Cu immobilised on the carbon surface.

Simulations using a simplified numerical model of a real swimming pool showed that progressive monochloramine conversion to N_2 in GAC filters significantly lowers the

concentration of inorganic chloramines and NDMA in pool water. The relative reduction of monochloramine and NDMA compared to the scenario without a GAC filter ranged from 0.5 to 2.7% for inorganic chloramines and from 1.7 to 4.5% for NDMA, depending on the type of GAC used. Also, model results indicated that the reduction of inorganic chloramines and NDMA in the pool could be increased by a factor of ~2 if the tested GACs could be modified so that their yields of monochloramine conversion to N_2 is ~50%.

6 Acknowledgements

Prof. Wladimir Reschetilowski, Prof. Martin Jekel and Dr. Irena Senkovska are thanked for their valuable discussions regarding the work presented in this study. Moreover, we thank Dr. Kathrin Gebauer and Dr. Arndt Weiske for performing the CNH and ICP-MS analysis. Jana Brückner and Gerit Orzechowski are acknowledged for their considerable continuous support in the laboratory. Veronika Zhiteneva is thanked for proof reading the manuscript. The authors would like to thank the anonymous reviewers for their helpful and constructive comments that greatly contributed to improving the final version of the paper. Mention of trade names, commercial products or services does not constitute endorsement or recommendation of use.

Abbreviations

CHN	Carbon, hydrogen and nitrogen (analyser)
CSTR1, CSTR2	Continuously stirred (completely mixed) tank reactors 1 and 2
DBP	Disinfection by-products
DMA	Dimethylamine
EBCT	Empty bed contact time
FBR	Fixed-bed reactor
GAC	Granular activated carbon
ICP-MS	Inductively coupled plasma mass spectrometry
LC-OCD-OND-UVD	Liquid chromatography with organic carbon, organic nitrogen und UV detection
MCA	Monochloramine
NDMA	N-nitrosodimethylamine

Symbols

$c_{bed,in}$	MCA in-flow concentrations of a GAC filter (mg L^{-1} as Cl_2)
$c_{bed,out}$	MCA out-flow concentrations of a GAC filter (mg L^{-1} as Cl_2)
c_{stock}	Concentration of the MCA stock solution (mg L^{-1} as Cl_2)
d_{60}	Sieve aperture size through which 60% (by mass) of activated carbon passes (in mm)

790 791	$N_{MCA}(t)$	Specific amount of monochloramine removed per g of GAC in the GAC filter until time t
792 793	$N_{NH4+}(t)$	Specific amount of ammonium formed per g of GAC in the GAC filter until time t
794 795	$N_{N2}(t)$	Specific amount of of nitrogen gas formed per g of GAC in the GAC filter until time t
796 797	$n_{NH4+,f}$	Mass flow of ammonia from the filling water of the nummerical swimming pool
798	$n_{urea,f}$	Mass flow of urea from the filling water of the nummerical swimming pool
799	$n_{DMA,f}$	Mass flow of DMA from the filling water of the nummerical swimming pool
800 801	$n_{NH4+,b}$	Mass flow of ammonia from the bathers of the nummerical swimming pool
802	$n_{urea,b}$	Mass flow of urea from the bathers of the nummerical swimming pool
803	$n_{DMA,b}$	Mass flow of DMA from the bathers of the nummerical swimming pool
804	k_{app}	Apparent -first-order reaction rate constant (s^{-1})
805	Q_{bed}	Volumetric fluid flow rate through a GAC bed (L s^{-1})
806	Q_{stock}	Volumetric dosing rate of an MCA stock solution (L s^{-1})
807	T	Temperature (K)
808	t_{EBCT}	Empty bed contact time (EBCT) (s)
809	V_{bed}	Bed volume (L)
810	v_{bed}	Superficial filter velocity (m s^{-1})
811	V_{sys}	Water volume in the FBR system (L)
812	Y_{NH4+}	Yield of NH_4^+ from monochloramine reduction

813	Y_{N2}	Yield of N_2 from monochloramine reduction
814	z_{bed}	Bed depth (m)

815

816 Greek symbols

817	ε	Molar absorption coefficient (mol^{-1} cm^{-1})
818	ζ	ζ-potential (mV)

819

References

Allwar, A., Characteristics of Pore Structures and Surface Chemistry of Activated Carbons by Physisorption, FTIR and Boehm Methods, Journal of Applied Chemistry, 2 (2012) 9–15.

ANSI/APSP-11-2009, American National Standard for Water Quality in Public Pools and Spa, The Association of Pool and Spa Professionals, Alexandria, 2009.

Aoki, T., Continuous-Flow Method for Simultaneous Determination of Monochloramine, Dichloramine, and Free Chlorine - Application to a Water-Purification Plant, Environmental Science and Technology, 23 (1989) 46–50.

Bauer, R.C., Snoeyink, V.L., Reactions of Chloramines with Active Carbon, Journal Water Pollution Control Federation, 45 (1973) 2290–2301.

Becker, F., Stetter, D., Janowsky, U., Overath, H., Abbau von Monochloraminen durch Aktivkohlefilter (in German), Gwf Wasser - Abwasser, 131 (1990) 1–8.

Bernard, A., Nickmilder, M., Voisin, C., Outdoor swimming pools and the risks of asthma and allergies during adolescence, European Respiratory Journal, 32 (2008) 979–988.

Bernard, A., Carbonnelle, S., Michel, O., Higuet, S., de Burbure, C., Buchet, J.P., Hermans, C., Dumont, X., Doyle, I., Lung hyperpermeability and asthma prevalence in schoolchildren: Unexpected associations with the attendance at indoor chlorinated swimming pools, Occupational and Environmental Medicine, 60 (2003) 385–394.

Blatchley, E.R., Cheng, M.M., Reaction Mechanism for Chlorination of Urea, Environmental Science and Technology, 44 (2010) 8529–8534.

Boehm, H.P., Chemical identification of surface groups, in: D.D. Eley, H. Pines, P. Weisz (Eds.) Advances in catalysis, Academic Press, New York/London, 1966.

Böhringer, B., Gonzalez, O.G., Eckle, I., Müller, M., Giebelhausen, J.-M., Schrage, C., Fichtner, S., Polymer-based Spherical Activated Carbons – From Adsorptive Properties to Filter Performance, Chemie Ingenieur Technik, 83 (2011) 53–60.

Branton, P.J., McAdam, K.G., Duke, M.G., Liu, C.A., Curle, M., Mola, M., Proctor, C.J., Bradley, R.H., Use of Classical Adsorption Theory to Understand the Dynamic Filtration of Volatile Toxicants in Cigarette Smoke by Active Carbons, Adsorption Science and Technology, 29 (2011) 117–138.

Cagnon, B., Py, X., Guillot, A., Joly, J.P., Berjoan, R., Pore structure modification of pitch-based activated carbon by NaOCl and air oxidation/pyrolysis cycles, Microporous Mesoporous Materials, 80 (2005) 183–193.

Chingombe, P., Saha, B., Wakeman, R.J., Surface modification and characterisation of a coal-based activated carbon, Carbon, 43 (2005) 3132–3143.

Choi, J.H., Valentine, R.L., Formation of N-nitrosodimethylamine (NDMA) from reaction of monochloramine: A new disinfection by-product, Water Research, 36 (2002) 817–824.

Cloteaux, A., Gérardin, F., Midoux, N., Numerical simulation and modelling of a typical swimming pool for disinfection by-products assessment, in: Fifth

862 International Conference Swimming Pool & Spa, Istituto Superiore di Sanità,
863 Rome, Italy, 2013, 117–127.

864 DIN 19643-1, Treatment of water of swimming pools and baths, Part 1: General
865 requirements (in German: Aufbereitung von Schwimm- und Badebeckenwasser,
866 Teil 1: Allgemeine Anforderungen), Normenausschuss Wasserwesen (NAW) im
867 DIN Deutsches Institut für Normung, Beuth Verlag, Berlin, 2012.

868 DIN 19643-2, Treatment of water of swimming pools and baths, Part 2: Combinations
869 of process with fixed bed filters and precoat filters (in German: Aufbereitung von
870 Schwimm- und Badebeckenwasser, Teil 2: Verfahrenskombinationen mit
871 Festbett- und Anschwemmfiltern), Normenausschuss Wasserwesen (NAW) im
872 DIN Deutsches Institut für Normung, Beuth Verlag, Berlin, 2012.

873 DIN 51724-3, Solid mineral fuels - Determination of sulfur content - Part 3:
874 Instrumental methods (in German: Prüfung fester Brennstoffe - Bestimmung
875 des Schwefelgehaltes - Teil 3: Instrumentelle Verfahren), Normenausschuss
876 Bergbau (FABERG) im DIN Deutsches Institut für Normung, Beuth Verlag,
877 Berlin, 2012.

878 DIN EN ISO-17294-2, Water quality - Application of inductively coupled plasma mass
879 spectrometry (ICP-MS) - Part 2: Determination of 62 elements (in German:
880 Wasserbeschaffenheit - Anwendung der induktiv gekoppelten Plasma-
881 Massenspektrometrie (ICP-MS) - Teil 2: Bestimmung von 62 Elementen),
882 Normenausschuss Wasserwesen (NAW) im DIN Deutsches Institut für
883 Normung, Beuth Verlag, Berlin, 2004.

884 DIN EN ISO 7393-2, Water quality - Determination of free chlorine and total chlorine,
885 Part 2: Colorimetric method using N,N-diethyl-1,4-phenylenediamine, for routine
886 control purposes (in German: Wasserbeschaffenheit - Bestimmung von freiem
887 Chlor und Gesamtchlor, Teil 2: Kolorimetrisches Verfahren mit N,N-Diethyl-1,4-
888 Phenylendiamin für Routinekontrollen), Normenausschuss Wasserwesen
889 (NAW) im DIN Deutsches Institut für Normung, Beuth Verlag, Berlin, 2000.

890 Edwards, M., Dudi, A., Role of chlorine and chloramine in corrosion of lead-bearing
891 plumbing materials, Journal of the American Water Works Association, 96
892 (2004) 69–81.

893 Eichelsdörfer, D., Slovak, J., Dirnagl, K., Schmid, K., The irritant effect (conjunctivitis)
894 of chlorine and chloramines in swimming pool water (in German: Zur
895 Reizwirkung (Konjunctivitis) von Chlor und Chloraminen im
896 Schwimmbeckenwasser), Vom Wasser, 45 (1975) 17–28.

897 Fairey, J.L., Speitel, G.E., Katz, L.E., Monochloramine destruction by GAC - Effect of
898 activated carbon type and source water characteristics, Journal of the American
899 Water Works Association, 99 (2007) 110–120.

900 Fairey, J.L., Speitel, G.E., Katz, L.E., Impact of natural organic matter on
901 monochloramine reduction by granular activated carbon: The role of porosity
902 and electrostatic surface properties. Environmental Science and Technology, 40
903 (2006) 4268–4273.

904 Fichtner, S., Adsorbents for various applications, Filtration and Speparation
905 International Edition, 10 (2010) 67–70.

906 Fu, J., Qu, J.H., Liu, R.P., Qiang, Z.M., Zhao, X., Liu, H., Mechanism of Cu(II)-
907 catalyzed monochloramine decomposition in aqueous solution, Science of the
908 Total Environment, 407 (2009) 4105–4109.

909 Gardner, T.H., Berry, D.A., Lyons, K.D., Beer, S.K., Freed, A.D., Fuel processor
910 integrated H_2S catalytic partial oxidation technology for sulfur removal in fuel
911 cell power plants, Fuel, 81 (2002) 2157–2166.

912 Ge, S., Wang, S., Yang, X., Qiu, S., Li, B., Peng, Y., Detection of nitrifiers and
913 evaluation of partial nitrification for wastewater treatment: a review,
914 Chemosphere, 140 (2015) 85–98.

915 Gérardin, F., Cloteaux, A., Midoux, N., Modeling of variations in nitrogen trichloride
916 concentration over time in swimming pool water, Process Safety and
917 Environmental Protection, 94 (2015) 452–462.

918 Goertzen, S.L., Theriault, K.D., Oickle, A.M., Tarasuk, A.C., Andreas, H.A.,
919 Standardization of the Boehm titration. Part I. CO(2) expulsion and endpoint
920 determination, Carbon, 48 (2010) 1252–1261.

921 Goifman, A., Gun, J., Gelman, F., Ekeltchik, I., Lev, O., Donner, J., Börnick, H.,
922 Worch, E., Catalytic oxidation of hydrogen sulfide by dioxygen on CoN4 type
923 catalyst, Applied Catalysis B: Environmental, 63 (2006) 296–304.

924 Hand, V.C., Margerum, D.W., Kinetics and Mechanisms of the Decomposition of
925 Dichloramine in Aqueous-Solution, Inorganic Chemistry, 22 (1983) 1449–1456.

926 Hassan, S., Yasin, T., Role of tailored surface of activated carbon for adsorption of
927 ionic liquids for environmental remediation, International Journal of
928 Environmental Science and Technology, 12 (2015) 2711–2722.

929 Hayden, R.A., Method for reactivating nitrogen-treated carbon catalysts, US patent
930 5.466.645, 1995.

931 Hua, G and Reckhow, D.A., Comparison of disinfection byproduct formation from
932 chlorine and alternative disinfectants, Water Research, 41 (2007) 1667-1678.

933 Huber, S.A., Balz, A., Abert, M., Pronk, W., Characterisation of aquatic humic and
934 non-humic matter with size-exclusion chromatography - organic carbon
935 detection - organic nitrogen detection (LC-OCD-OND), Water Research, 45
936 (2011a) 879–885.

937 Huber, S.A., Balz, A., Abert, M., New method for urea analysis in surface and tap
938 waters with LC-OCD-OND (liquid chromatography-organic carbon detection-
939 organic nitrogen detection), Journal of Water Supply Research and Technology-
940 Aqua, 60 (2011b) 159–166.

941 Isaac, R.A., Morris, J.C., Transfer of Active Chlorine from Chloramine to Nitrogenous
942 Organic-Compounds. 1. Kinetics, Environmental Science and Technology, 17
943 (1983) 738–742.

944 Jacangelo, J.G., Olivieri, V.P., Kawata, K., Oxidation of Sulfhydryl-Groups by
945 Monochloramine, Water Research, 21 (1987) 1339–1344.

946 Jafvert, C.T., Valentine, R.L., Reaction Scheme for the Chlorination of Ammoniacal
947 Water, Environmental Science and Technology, 26 (1992) 577–586.

948 Judd, S.J., Black, S.H, Disinfection by-product formation in swimming pool waters: A
949 simple mass balance, Water Research, 34 (2000) 1611–1619.

950 Jurado-Sanchez, B., Ballesteros, E., Gallego, M., Screening of N-nitrosamines in tap
951 and swimming pool waters using fast gas chromatography, Journal of
952 Separation Science, 33 (2010) 610–616.

953 Kalijadis, A.M., Vukcevic, M.M., Jovanovic, Z.M., Lausevic, Z.V., Lausevic, M.D.,
954 Characterisation of surface oxygen groups on different carbon materials by the
955 Boehm method and temperature-programmed desorption, Journal of the
956 Serbian Chemical Society, 76 (2011) 757–768.

957 Keuten, M.G.A., Peters, M.C.F.M., Daanen, H.A.M., de Kreuk, M.K., Rietveld, L.C.,
958 van Dijk, J.C., Quantification of continual anthropogenic pollutants released in
959 swimming pools, Water Research, 53 (2014) 259–270.

960 Keuten, M.G.A., Schets, F.M., Schijven, J.F., Verberk, J.Q.J.C., van Dijk, J.C.,
961 Definition and quantification of initial anthropogenic pollutant release in
962 swimming pools, Water Research, 46 (2012) 3682–3692.

963 Kim, B.R., Analysis of batch and packed bed reactor models for the carbon-
964 chloramine reactions, Doctoral thesis, University of Illinois at Urbana-
965 Champaign, Illinois, 1977.

966 Kim, B.R., Snoeyink, V.L., The Monochloramine-GAC Reaction in Adsorption
967 Systems, Journal of the American Water Works Association, 72 (1980) 488–
968 490.

969 Kim, B.R., Snoeyink, V.L., Schmitz, R.A., Removal of dichloramine and ammonia by
970 granular carbon, Journal Water Pollution Control Federation, 50 (1978) 122–
971 133.

972 Kochany, J. and Lipczynska-Kochany, E., Catalytic Destruction of Chloramine to
973 Nitrogen Using Chlorination and ActivatedCarbon - Case Study, Water
974 Environment Research, 80 (2008) 339–345.

975 Lee, M.J., Lee, Y.H., Soltermann, F., von Gunten, U., Analysis of N-nitrosamines and
976 other nitro(so) compounds in water by high-performance liquid chromatography
977 with post-column UV photolysis/Griess reaction, Water Research, 47 (2013)
978 4893–4903.

979 Liu, Z.S., Chen, J.Y., Peng, Y.H., Activated carbon fibers impregnated with Pd and Pt
980 catalysts for toluene removal, Journal of Hazardous Materials, 256 (2013) 49–
981 55.

982 Matviya, T.M., Hayden, R.A., Catalytic carbon, US patent 5.356.849, 1994.

983 Menendez-Diaz, J. A., Martin-Gullon, I., Types of carbon adsorbents and their
984 production, Interface Science and Technology, 7 (2006) 1–48.

985 Memendez, J.A, Illan-Gomez, M.J., Leon y Leon, C.A., Radovic, L.R., On the
986 difference between the isoelectric point and the point of zero charge of carbons,
987 Carbon, 33 (1995) 1655-1659.

988 Mitch, W.A., Sedlak, D.L., Formation of N-nitrosodimethylamine (NDMA) from
989 dimethylamine during chlorination, Environmental Science and Technology, 36
990 (2002) 588–595.

991 Oickle, A.M., Goertzen, S.L., Hopper, K.R., Abdalla, Y.O., Andreas, H.A.,
992 Standardization of the Boehm titration: Part II. Method of agitation, effect of
993 filtering and dilute titrant, Carbon, 48 (2010) 3313–3322.

994 Perrard, A., Retailleau, L., Berjoan, R., Joly, J.P., Liquid phase oxidation kinetics of
995 an ex-cellulose activated carbon cloth by NaOCl, Carbon, 50 (2012) 2226–
996 2234.

997 Qiang, Z.M., Adams, C.D., Determination of monochloramine formation rate
998 constants with stopped-flow spectrophotometry, Environmental Science and
999 Technology, 38 (2004) 1435–1444.

1000 Raave, H., Keres, I., Kauer, K., Noges, M., Rebane, J., Tampere, M., Loit, E., The
1001 impact of activated carbon on NO3--N, NH4+-N, P and K leaching in relation to
1002 fertilizer use, European Journal of Soil Science, 65 (2014) 120–127.

1003 Reichert, P., Aquasim - a tool for simulation and data-analysis of aquatic systems,
1004 Water Science and Technology, 30 (1994) 21–30.

1005 Sakuma, M. , Matsushita, T., Matsui, Y., Aki, T., Isaka, M., Shirasaki, N.,
1006 Mechanisms of trichloramine removal with activated carbon: Stoichiometric
1007 analysis with isotopically labeled trichloramine and theoretical analysis with a
1008 diffusion-reaction model, Water Research, 68 (2015) 839–848.

1009 Scaramelli, A.B., Digiano, F.A., Effect of sorbed organics on efficiency of ammonia
1010 removal by chloramine-carbon surface-reactions, Journal Water Pollution
1011 Control Federation, 49 (1977) 693–705.

1012 Schmalz, C., Frimmel, F.H., Zwiener, C., Trichloramine in swimming pools -
1013 Formation and mass transfer, Water Research, 45 (2011) 2681–2690.

1014 Schreiber, I.M., Mitch, W.A., Nitrosamine formation pathway revisited: The
1015 importance of chloramine speciation and dissolved oxygen, Environmental
1016 Science and Technology, 40 (2006) 6007–6014.

1017 Schreiber, I.M., Mitch, W.A., Influence of the order of reagent addition on NDMA
1018 formation during chloramination, Environmental Science and Technology, 39
1019 (2005) 3811–3818.

1020 Schurter, L.M., Bachelor, P.P., Margerum, D.W., Nonmetal Redox Kinetics -
1021 Monochloramine, Dichloramine, and Trichloramine Reactions with Cyanide Ion,
1022 Environmental Science and Technology, 29 (1995) 1127–1134.

1023 Sevilla, M., Fuertes, A.B., Mokaya, R., High density hydrogen storage in
1024 superactivated carbons from hydrothermally carbonized renewable organic
1025 materials, Energy and Environmental Science, 4 (2011) 1400–1410.

1026 SIA 385/9, Water and water treatment in public pools (in German: Wasser und
1027 Wasseraufbereitungsanlagen in Gemeinschaftsbädern), Swiss society of
1028 engineers and architects (SIA), Zürich, 2011.

1029 Skibinski, B., Goetze, C., Worch, E., Uhl, W., Pore diffusion limits removal of
1030 monochloramine in treatment of swimming pool water using granular activated
1031 carbon, Water Research, 132 (2018) 270–281.

1032 Snoeyink, V.L., Lai, H.T., Johnson, J.H., Young, J.F., Active carbon: Dechlorination
1033 and the adsorption of organic compounds, in: A. Rubin (Ed.) Chemistry of Water
1034 Supply, Treatment and Distribution, Ann Arbor Science Publishers, Ann Arbor,
1035 1974.

1036 Soltermann, F., Lee, M., Canonica, S., von Gunten, U., Enhanced N-nitrosamine
1037 formation in pool water by UV irradiation of chlorinated secondary amines in the
1038 presence of monochloramine, Water Research, 47 (2012) 79–90.

1039 Strelko, V., Malik, D.J., Streat, M., Characterisation of the surface of oxidised carbon
1040 adsorbents, Carbon, 40 (2002) 95–104.

1041 Suidan, M.T., Snoeyink, V.L., Schmitz, R.A., Reduction of Aqueous Free Chlorine
1042 with Granular Activated Carbon, pH and Temperature Effects, Environmental
1043 Science and Technology, 11 (1977a) 785–789.

1044 Suidan, M.T., Snoeyink, V.L., Schmitz, R.A., Reduction of Aqueous HOCl with
1045 Activated Carbon, Journal of Environmental Engineering Division ASCE, 103
1046 (1977b) 677–691.

1047 Suidan, M.T., Snoeyink, V.L., Thacker, W.E., Dreher, D.W., Influence of Pore-Size
1048 Distribution on Hocl-Activated Carbon Reaction, Abstracts of Papers of the
1049 American Chemical Society, 173 (1977c) 66–66.

1050 Sun, Y., Webley, P.A., Preparation of activated carbons from corncob with large
1051 specific surface area by a variety of chemical activators and their application in
1052 gas storage, Chemical Engineering Journal, 162 (2010) 883–892.

1053 Switzer, J.A., Rajasekharan, V.V., Boonsalee, S., Kulp, E.A., Bohannan, E.W.,
1054 Evidence that monochloramine disinfectant could lead to elevated Pb levels in
1055 drinking water, Environmental Science and Technology, 40 (2006) 3384–3387.

1056 Sze, A., Erickson, D., Ren, L.Q., Li, D.Q., Zeta-potential measurement using the
1057 Smoluchowski equation and the slope of the current-time relationship in
1058 electroosmotic flow, Journal of Colloid and Interface Science, 261 (2003) 402–
1059 410.

1060 Tsai, W.T., Chang, C.Y., Surface-Chemistry of Activated Carbons and Its Relevance
1061 for Effects of Relative-Humidity on Adsorption of Chlorinated Organic Vapors,
1062 Chemosphere, 29 (1994) 2507–2515.

1063 Uhl, W., Hartmann, C., Disinfection by-products and microbial contamination in the
1064 treatment of pool water with granular activated carbon. Water Science &
1065 Technology, 52 (2005) 71–76.

1066 Valentine, R.L., Brandt, K.I., Jafvert, C.T., A Spectrophotometric Study of the
1067 Formation of an Unidentified Monochloramine Decomposition Product, Water
1068 Research, 20 (1986) 1067–1074.

1069 Vikesland, P.J., Valentine, R.L., Iron oxide surface-catalyzed oxidation of ferrous iron
1070 by monochloramine: Implications of oxide type and carbonate on reactivity,
1071 Environmental Science and Technology, 36 (2002) 512–519.

1072 Wang, J.C., Senkovska, I., Kaskel, S., Liu, Q., Chemically activated fungi-based
1073 porous carbons for hydrogen storage, Carbon, 75 (2014) 372–380.

1074 Weaver, W.A., Li, J., Wen, Y.L., Johnston, J., Blatchley, M.R., Blatchley, E.R.,
1075 Volatile disinfection by-product analysis from chlorinated indoor swimming
1076 pools, Water Research, 43 (2009) 3308–3318.

1077 Weil, I., Morris, C., Kinetic Studies on the Chloramines. I. The Rates of Formation of
1078 Monochloramine, N-Chlormethylamine and N-Chlordimethylamine, Journal of
1079 the American Chemical Society, 71 (1949) 1664–1671.

1080 Wojtowicz, J. A., Chemistry of Nitrogen Compounds in Swimming Pool Water,
1081 Journal of the Swimming Pool and Spa Industry, 4 (2001) 30–49.

1082 World Health Organisation (WHO), Guidelines for safe recreational water
1083 environments, Volume 2: Swimming Pools and Similar Environments, WHO,
1084 Geneva, 2006.

1085 Worch, E., Adsorption Technology in Water Treatment: Fundamentals, Processes,
1086 and Modeling, Walter de Gruyter GmbH & Co. KG, Berlin/Boston, 2012.

1087 Xiang, Z., Dai Q., Chen, J.F., Dai, L., Edge functionalization of graphene and two-
1088 dimensional covalent organic polymers for energy conversion and storage,
1089 Advanced Materials, 28 (2016) 6253–6261.

1090 Zhang, H., Zhang, K., Jin, H., Gu, L., Yu, X, Variations in dissolved organic nitrogen
1091 concentration in biofilters with different media during drinking water treatment,
1092 Chemosphere, 139 (2015) 652–658.

1093 Zhang, B., Wen, Z.H., Ci, S.Q., Chen, J.H., He, Z., Nitrogen-doped activated carbon
1094 as a metal free catalyst for hydrogen production in microbial electrolysis cells,
1095 RSC Advances, 4 (2014a) 49161–49164.

1096 Zhang, B., Wen, Z.H., Ci, S.Q., Mao, S., Chen, J.H., He, Z., Synthesizing Nitrogen-
1097 Doped Activated Carbon and Probing its Active Sites for Oxygen Reduction
1098 Reaction in Microbial Fuel Cells, ACS Applied Materials Interfaces, 6 (2014b)
1099 7464–7470.

1100 Zhang, X.H., Pehkonen, S.O., Kocherginsky, N., Ellis, G.A., Copper corrosion in
1101 mildly alkaline water with the disinfectant monochloramine, Corrosion Science,
1102 44 (2002) 2507–2528.

1103 Zwiener, C., Richardson, S.D., De Marini, D.M, Grummt, T., Glauner, T., Frimmel,
1104 F.H., Drowning in disinfection byproducts? Assessing swimming pool water,
1105 Environmental Science and Technology, 41 (2007) 363–372.

1106

Tables

Table 1: Operation conditions of the laboratory-scale plant.

Parameter	**Value**
Column diameter, d_{bed}	34 mm
Bed volume, V_{bed}	32 mL
Fluid flow, Q_{bed}	40 L h^{-1}
Contact time	2.88 s
Temperature, T	30 °C
Monochloramine concentration, $c_{bed,in}$	4.5 (mg L^{-1} (as Cl_2))
pH	7

1111 Table 2: Concentration of acidic oxygen groups on the surface of the fresh and altered GACs and correlation analysis for the
1112 dependence of N_2 yield on the acidic oxygen surface groups.

Carbon	Concentration of acidic surface functionalities in µmol g_{GAC}^{-1} [a]											
	Total			Phenolic			Lactonic			Carboxylic		
	fresh	altered	formed	fresh	altered	formed	fresh	altered	formed	fresh	altered	formed
30N	1758	2036	282	0	76	76	62	155	93	1696	1805	109
K835	1795	2163	368	51	96	45	152	212	60	1592	1855	263
Centaur	1926	2167	240	43	110	67	105	208	103	1778	1849	71
100058	1728	2092	364	8	75	67	51	173	122	1670	1844	174
r	-0.21	0.55	0.84	0.57	0.13	-0.94	0.65	0.58	-0.53	-0.82	0.73	0.94

1113 [a] The standard method deviations of the concentration of acidic oxygen groups were as follows: 75 µmol g_{GAC}^{-1} (Total), 15 µmol g_{GAC}^{-1} (phenolic), 76 µmol g_{GAC}^{-1} (lactonic), 55
1114 µmol g_{GAC}^{-1} (carboxylic) (n=8).
1115

Table 3: Elemental analysis of the tested GACs and correlation analysis for the dependence of N_2 yield on the elemental composition.

Carbon	N_2 yield in % [a]	Elemental analysis in g g_{GAC}^{-1}				Trace metal concentration in µg g_{GAC}^{-1}						
		C	N	H	S	Fe	Mn	Co	Ni	Cu	Rh	Pd
blank		n.d.	n.d.	n.d.	n.d.	8.3	0.05	n.d.	n.d.	0.4	n.d.	n.d.
K835	21.3±4.1	86.0±0.0	0.2±0.02	1.2±0.03	0.1±0.00	32±13	8.1±0.3	0.04±0.0	0.9±0.3	14.1±0.4	n.d.	0.004±0.001
100058	11.6±3.0	96.9±0.0	0.1±0.01	0.5±0.00	1.4±0.03	2483±349	47.5±11.5	1.1±3.5	74.8±0.0	10.9±2.7	n.d.	0.004±0.010
Centaur	4.2±3.0	81.5±4.1	0.7±0.14	1.4±0.03	0.8±0.01	172±50	2.5±0.9	2.2±0.3	9.4±2.9	10.2±2.0	n.d.	0.050±0.005
30N	0.5±4.7	84.6±0.3	0.3±0.00	0.8±0.02	0.4±0.01	4306±216	90.5±11.2	9.2±1.0	16.0±0.1	6.8±0.3	n.d.	0.083±0.007
r		0.32	0.55	0.03	0.26	-0.59	-0.55	-0.80	-0.02	0.95	-	-0.89

n.d. … None detected

[a] … Errors represent the standard deviation (n = 2)

1120 **Figures**

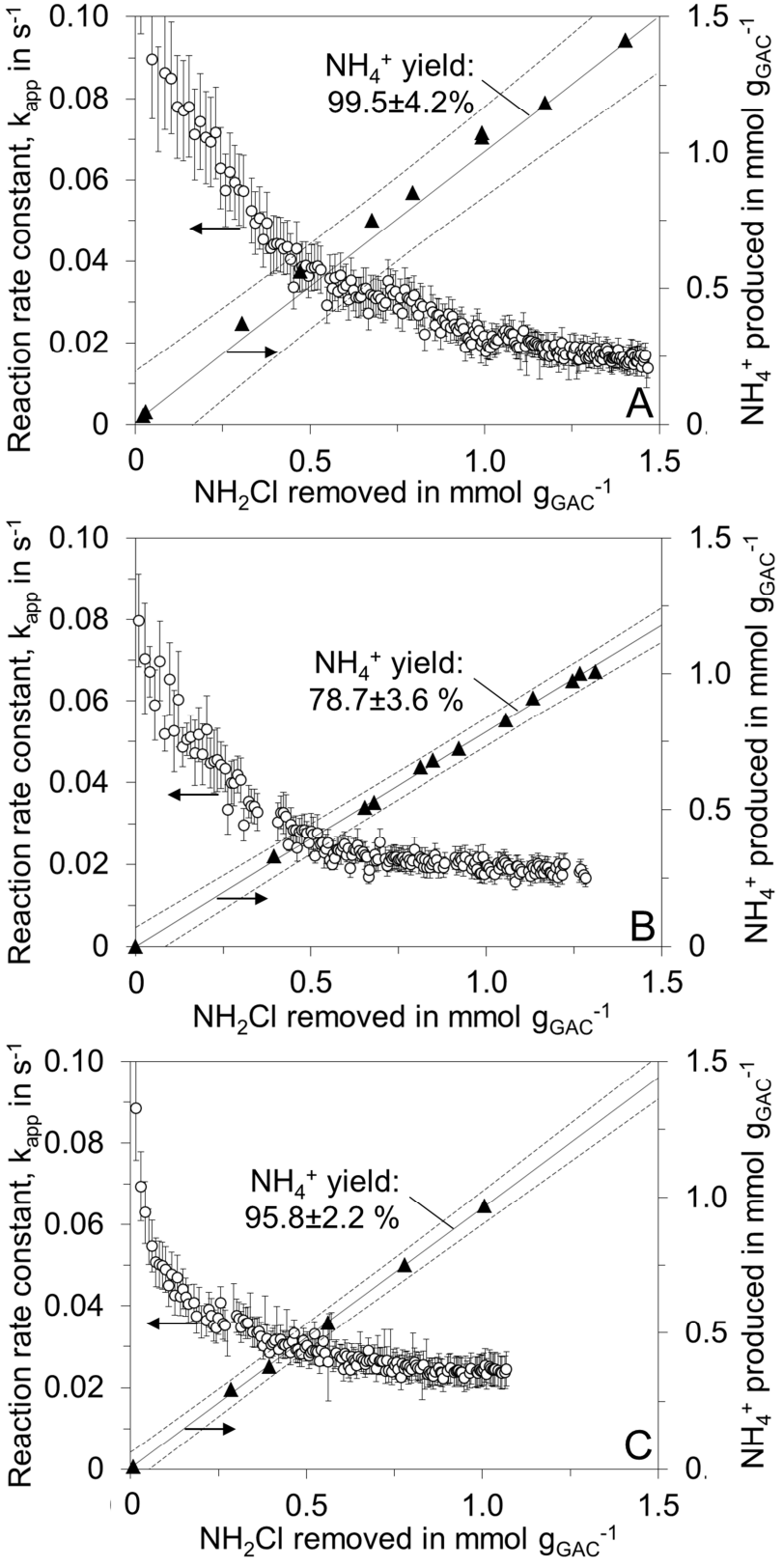

1121
1122

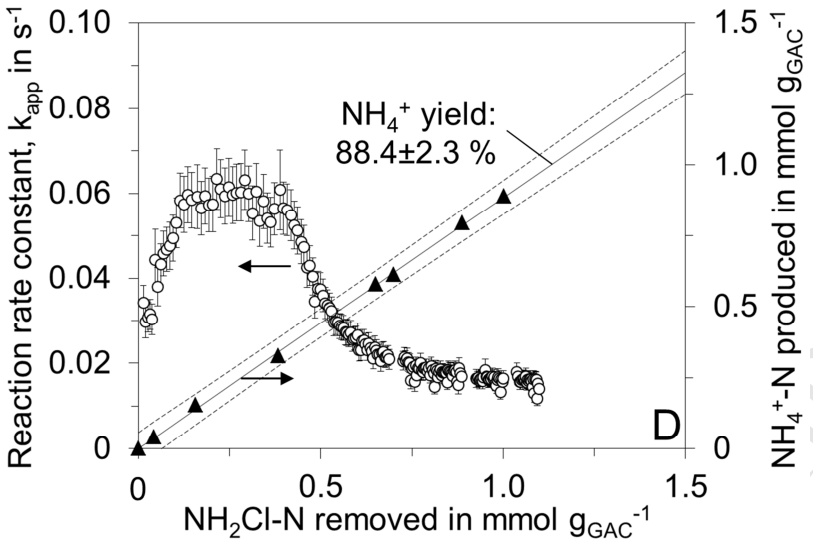

Figure 1: Reaction rate constant and specific amount of NH_4^+ produced per g GAC versus the specific amount of monochloramine removed per g of GAC for the 30N (A), K835 (B), Centaur (C) and 100058 (D) GACs. Error bars for k_{app} represent the standard deviation (n = 20). Solid lines represent the linear least-squares best fit of the correlation between monochloramine removed and NH_4^+ produced. Dashed lines represent the corresponding 95% confidence band of the fitted regression. The NH_4^+ yields from monochloramine removal were derived from the slope of the linear regressions. Errors of the NH_4^+ yield represent the error of the slope of the linear correlation.

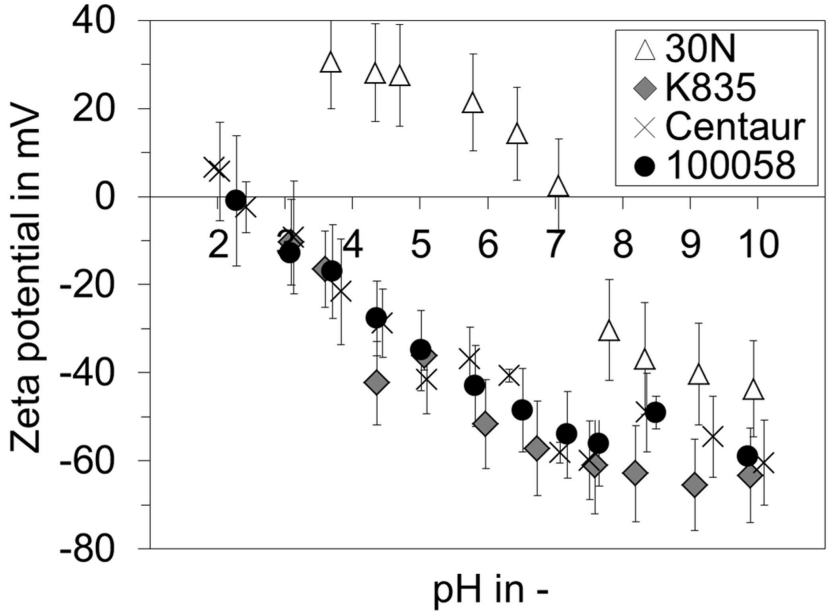

1134

1135 Figure 2: Zeta potentials of the fresh 100058, 30N, K835 and Centaur GACs at
1136 different pH. Error bars represent the standard deviation of three
1137 repeated experiments.

1138

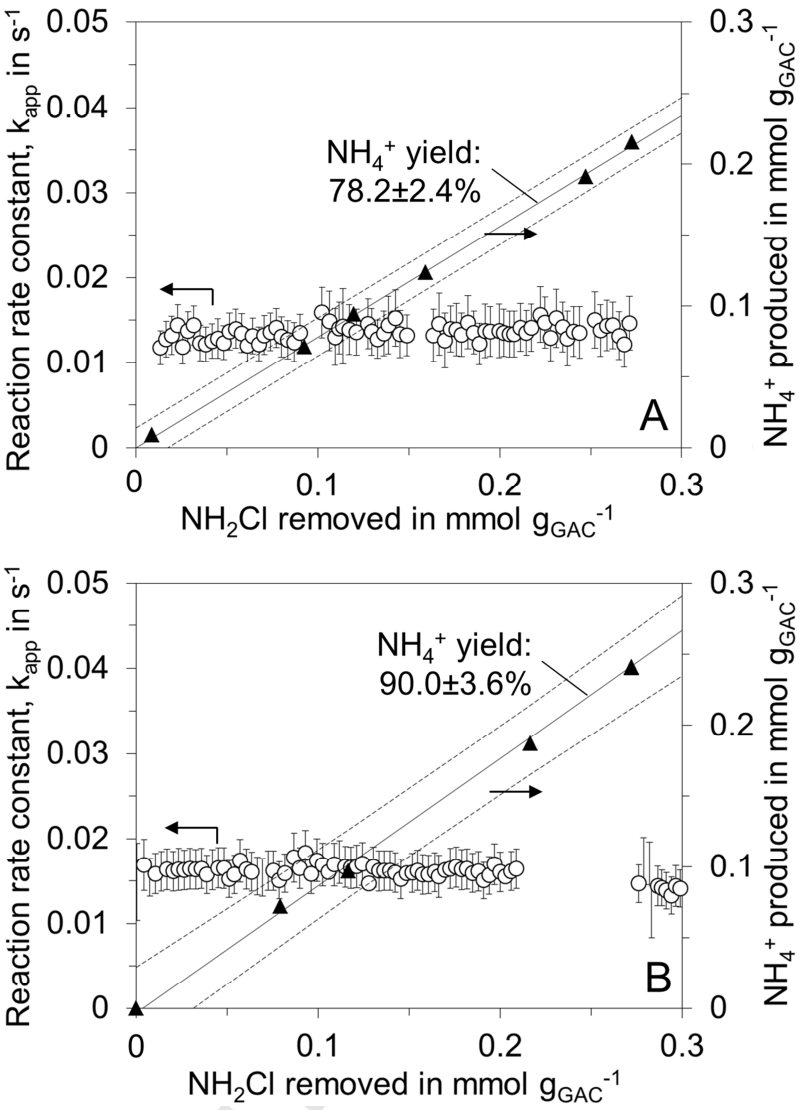

1139

1140 Figure 3: Reaction rate constant k_{app} and specific amount of NH_4^+ produced
1141 per g GAC plotted against the specific amount of monochloramine
1142 degraded per g GAC for the K835 (A) and Centaur (B) GACs after
1143 HOCl pre-treatment. Error bars for k_{app} represent the standard
1144 deviation (n = 20). Solid lines represent the linear least-squares best
1145 fit of the correlation between monochloramine removed and NH_4^+
1146 produced. Dashed lines represent the corresponding 95% confidence
1147 band of the fitted regression. Errors in the NH_4^+ yield represent the
1148 errors in the slope of the linear correlation. Interruptions in the k_{app}
1149 curve were caused by imperfect data acquisition.

1150

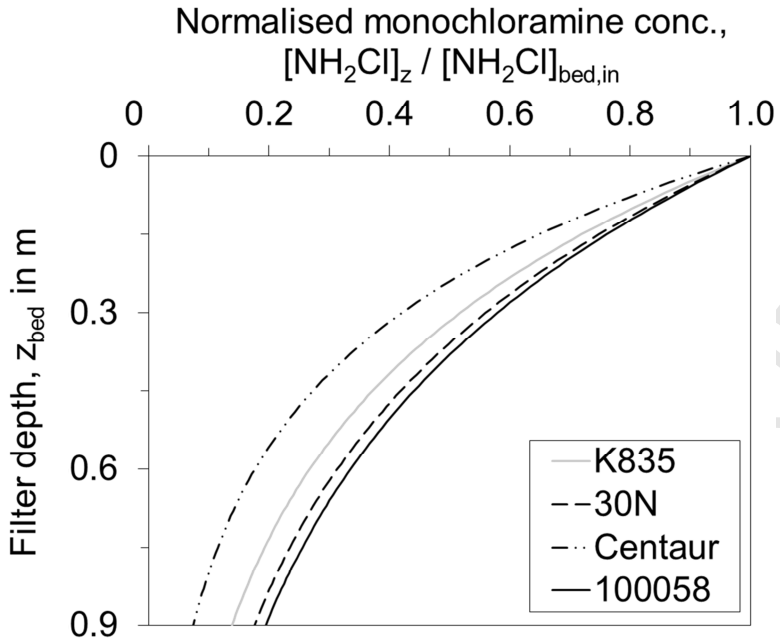

1151

1152 Figure 4: Simulated normalised monochloramine concentrations over the bed
1153 depth of a theoretical GAC filter (z_{bed} = 0.9 m) for the K835, 30N,
1154 Centaur and 100058 GACs. Concentration profiles were calculated
1155 according to Equation C.1 (SM) using a v_{eff} of 30 m h^{-1}. The reaction
1156 rate constants used for calculation were those observed when
1157 stationary conditions were reached (see Figure 1).

1158

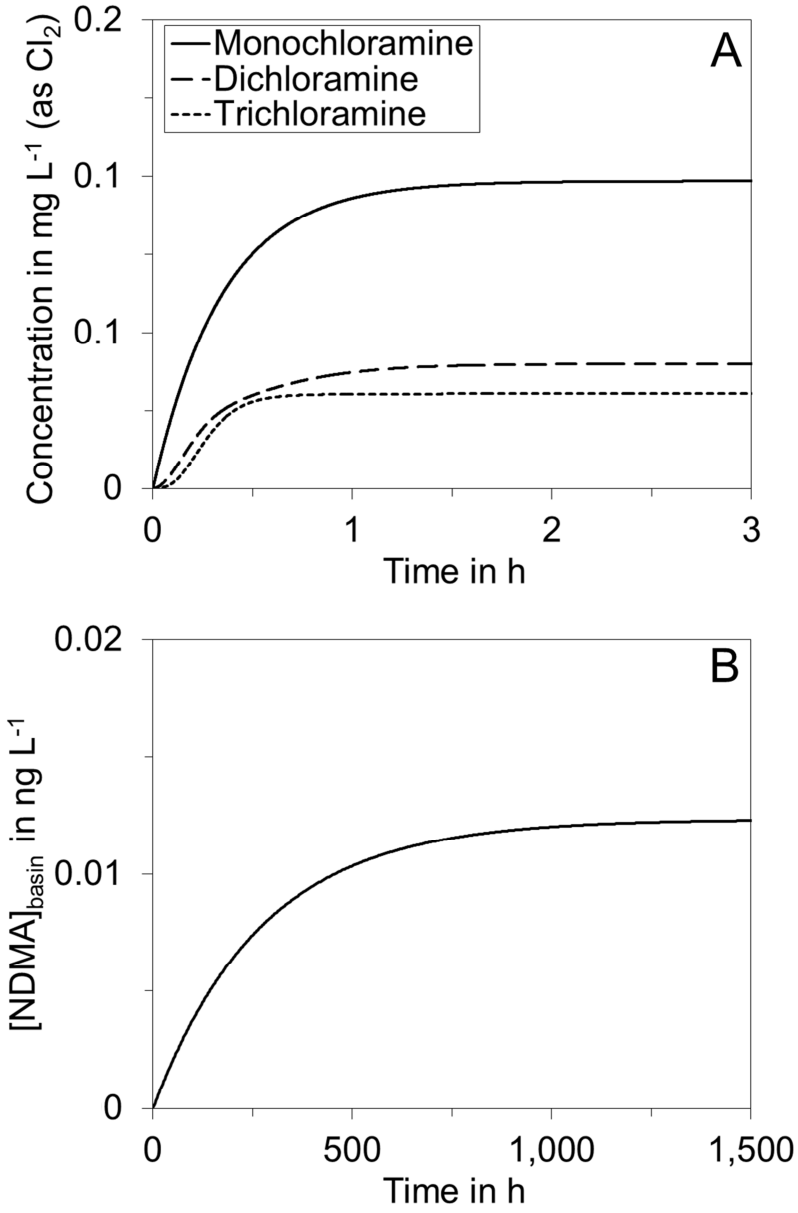

Figure 5: Evolution of simulated concentrations of mono-, di- and trichloramine (A) and NDMA (B) in the simplified numerical pool model. As an illustrative example, the carbon reactivity k_{app} and N_2 yield of the carbon were chosen to be that of the K835 carbon (k_{app} = 0.0183 s^{-1}, N_2 yield = 21.3 %).

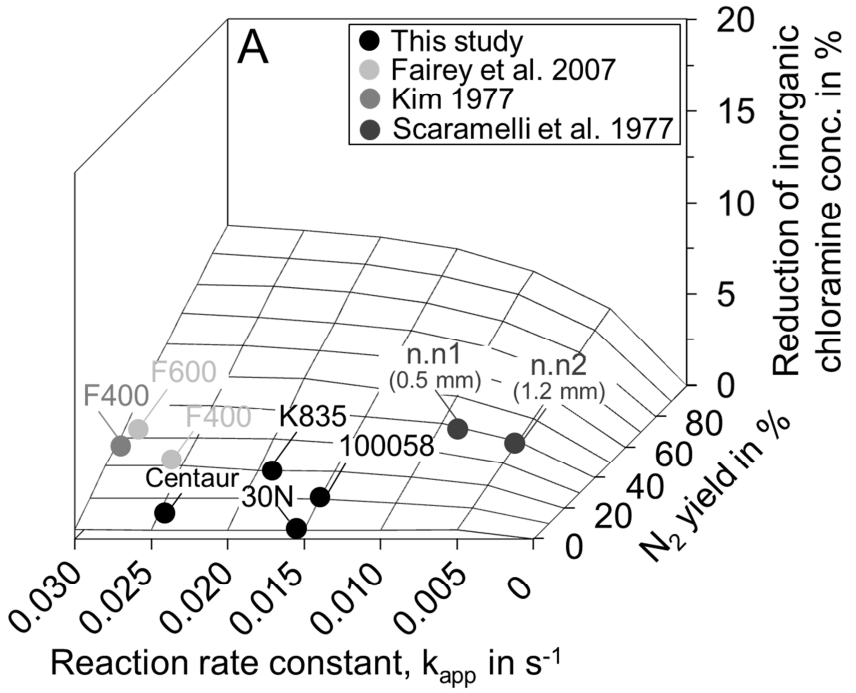

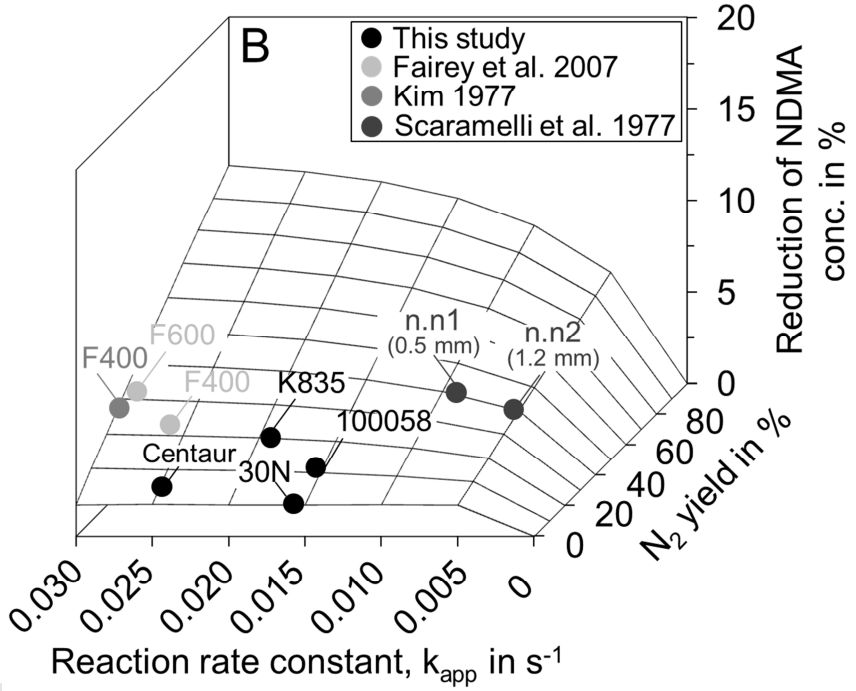

1167

1168 Figure 6: Impact of k_{app} and N_2 yield on stationary concentrations of inorganic
1169 chloramines and NDMA as simulated using the simplified numerical
1170 swimming pool model. Results are displayed as the relative
1171 normalised reduction relatedconcentration reduction when related to
1172 the scenario without a GAC filter

Highlights

- N_2 yields from monochloramine conversion by GAC were determined
- Conditions were typical for swimming pool water treatment
- Oxygen groups present on the GAC surface do not affect the N_2 yield
- Correlation between amount of Cu found in GACs and N_2 yields
- Using carbons with high N_2 yield improves swimming pool water quality

Declaration of interests

☒ The authors declare that they have no known competing financial interests or personal relationships that could have appeared to influence the work reported in this paper.

☐The authors declare the following financial interests/personal relationships which may be considered as potential competing interests: